BNWL-1712

A STUDY OF SOIL WATER POTENTIAL AND TEMPERATURE IN HANFORD SOILS

by

J. J. C. Hsieh
A. E. Reisenauer
L. E. Brownell*

Water and Land Resources Department
*Atlantic Richfield Hanford Company

1973

This report is based on work sponsored by the Atlantic Richfield Hanford Company under United States Atomic Energy Commission Contract AT(45-1)-2130

BATTELLE
PACIFIC NORTHWEST LABORATORIES
RICHLAND, WASHINGTON 99352

SUMMARY

This document describes in detail the construction and installation of a string of thermocouple psychrometers and diode temperature transducers in the soil between the soil surface and the groundwater table on the Hanford Reservation. The results of fifteen months of data gathering from these instruments indicate that moisture movement in the soil profile, if any, is extremely small.

CONTENTS

FIGURES

TABLES

A STUDY OF SOIL WATER POTENTIAL AND TEMPERATURE IN HANFORD SOILS

INTRODUCTION

A knowledge of the movement of precipitation water in the arid soil of the Hanford Reservation is important in the evaluation of long-term waste management practices at the Reservation. Research has been carried out in conjunction with Atlantic Richfield Hanford Company for the Atomic Energy Commission to gain such knowledge. Wells have been drilled and hydraulic characteristic and vapor equilibrium measurements have been made on soil samples taken from these wells in an effort to obtain conclusive information about subsurface rainfall movement. Tritium measurements were also made on the moisture contained in the soil samples and the wells were logged with a neutron probe. However, inconclusive results were obtained from these studies and it was not possible to determine conclusively whether moisture derived from precipitation would eventually migrate to the water table.

To provide more definitive results, a new approach was initiated using the energy status of the moisture in the soil profile to quantify the total water flux. The total water flux is a function of the water potential and thermal gradients and requires treatment of both the vapor and liquid phases. The water potential can be decomposed into the following components:

$$\psi_w = \psi_s + \psi_p + \psi_m + \psi_g \qquad (1)$$

where

ψ_w = total water potential

ψ_s = osmotic (solute) potential

ψ_p = pneumatic (pressure) potential

ψ_m = matric (capillary) potential

ψ_g = gravitational potential

The ψ_p term is small in almost all instances and is considered negligible.

It can be seen from the above equation that the water potential is a function of the moisture content and hydraulic characteristic of the sediments (ψ_m) as well as temperature. This use of the energy approach to compute the total water flux requires reliable data on water potentials, temperatures and the hydraulic characteristics of the sediments for the entire soil profile.

To provide the data necessary to use the energy approach, in August of 1970 a well was drilled from the ground surface to the groundwater table at a location about 1 mile south of 200 East Area. Soil samples were taken from this well to determine the hydraulic characteristics of the various sediment horizons which make up the vertical profile. An instrumented cable of thermocouple psychrometers (TCP) and diode temperature transducers (DTT) was installed at specific intervals in the well hole. These instruments will provide the additional information on water potentials and temperatures necessary to use the energy approach. The psychrometers will measure the ψ_s and ψ_m components of the total water potential (Equation 1). The osmotic potentials should be small since the soils in question are nonsaline. Thus for ease of discussion, the psychrometer readings will be considered a direct measurement of the matric potential. The other component of the total water potential (ψ_g) can be readily determined if the elevation of the psychrometer with respect to a given datum (usually mean sea level) is known. A more detailed discussion of water potential is contained in Appendix A.

Once reliable data are obtained from the above system, the direction of net moisture movement at any depth can be calculated and subsequently used to infer the percolation depth of precipitation water. Since installation, the instrumented cable has been monitored twice weekly; the monthly averages are reported in this document.

CLIMATOLOGICAL DATA

Climatological data used in this research are based on records compiled by the Hanford Meteorology Station from 1945-1970, supplemented with precipitation and temperature data of the United States Weather Bureau cooperative observers at a nearby site from 1912 to 1944.

The Hanford Meteorology Station operated by Battelle-Northwest is situated on a plateau in south central Washington about 5 miles northwest of the instrument site. The plateau slopes down toward the Columbia River about 10 miles north of the station and up to the foothills of Rattlesnake Mountain about 10 miles south of the station. Elevation of the station is 733 feet, which is roughly 300 feet above the Columbia River.

Since the Hanford Reservation is in the rain shadow of the Cascade Mountains, precipitation totals only 6.25 inches annually. The three months of November through January contribute 42 percent of this total, while the three months of July through September contribute only 10 percent. There are only two occurrences per year of 24-hour amounts of 0.50 inch or more. About 45 percent of all precipitation during the months of December through February is in the form of snow. There have been 81 consecutive days without measurable rain (June 22 - September 10, 1967), 139 days with only 0.18 inch (June 22 - November 7, 1967), and 172 days with only 0.32 inch (February 24 - August 13, 1968).

By serving as a source of cold air drainage, the Cascade Mountains also have a considerable effect on the wind regime at Hanford. This drainage (gravity) wind, plus topographic channeling, causes a considerable diurnal range of wind speed during the summer. In July, hourly average speeds range from a low of 5.2 mph from 9:00 a.m. to 10:00 a.m. to a high of 13.0 mph from 9:00 p.m. to 10:00 p.m. In contrast, the corresponding speeds for January are 5.5 and 6.3 mph.

Temperatures at the Hanford Reservation are colder in winter and warmer in summer than they would be without the Cascade Mountains. However, other mountain ranges shield the area from many of the arctic air mass surges. Hanford experiences many warm, cloudless days and as a result the solar radiation is consistently high.

Although winter temperature minima have varied from -27°F to +22°F, summer maxima have varied only from 100°F to 115°F. However, there is considerable variation in the frequency of such maxima.

Weather data during the experimental period are reported in Tables 1, 2 and 3. Table 1 shows monthly precipitation and relative humidity data, which are average for this period.

Table 1. WEATHER DATA DURING THE STUDY

February 1971 to April 1972

	PRECIPITATION (IN.)							RELATIVE HUMIDITY (%)	
						Snow, Ice Pellets			
	Month	Total	Departure	Greatest in 24 Hours	Date	Total	Departure	Average	Departure
1971	J	0.78	-0.20	0.53	16	2.0	-3.3	72	-4
	F	0.10	-0.53	0.06	9	T	-1.8	62	-8
	M	1.02	+0.54	0.51	25-26	0.6	+0.1	56	0
	A	0.07	-0.30	0.06	24	0	0	43	-4
	M	0.56	+0.06	0.36	30-31	0	0	37	-5
	J	0.71	+0.14	0.39	2-3	0	0	41	+1
	J	0.13	-0.01	0.13	9	0	0	27	-5
	A	0.09	-0.10	0.09	22	0	0	30	-5
	S	1.13	+0.83	0.52	1-2	0	0	45	+4
	O	0.18	-0.40	0.16	29-30	0.6	+0.6	51	-7
	N	0.46	-0.39	0.12	11-12	T	-1.1	73	0
	D	1.07	+0.21	0.32	8	8.1	+4.0	78	-2
1971		6.30	-0.15	0.53	Jan 16	11.3	-1.5	51	-3.5
1972	J	0.19	-0.78	0.09	23-24	4.9		69.8	
	F	0.27	-0.31	0.09	4-5	1.4		75.4	
	M	0.58	+0.20	0.22	12	0.1		61.3	
	A	0.10	-0.34	0.08	11.1	T		43.0	

Table 2 shows the temperature and mean sky cover for the test period which again is near the long-term average.

Table 2. TEMPERATURE AND MEAN SKY COVER

February 1971 to April 1972

		TEMPERATURE (°F)								MEAN SKY COVER[1] (Tenths)	
		Averages				Extreme					
	Month	Daily Maximum	Daily Minimum	Monthly	Departure	Highest	Date	Lowest	Date	Average	Departure
1971	J	45.0	26.0	35.8	+6.2	72	31	8	4	8.1	+0.3
	F	49.7	28.5	39.1	+3.6	66	13	15	6	7.0	-0.4
	M	52.1	29.3	40.7	-3.7	65	29	15	2+	7.1	+0.4
	A	65.4	38.6	52.0	-1.4	76	6	27	1	6.7	+0.3
	M	77.9	50.2	64.0	+1.7	92	12	36	20	6.0	+0.2
	J	78.7	51.8	65.3	-4.1	99	22	44	8	6.6	+1.4
	J	94.6	62.7	78.7	+2.3	111	31	44	6	2.5	-0.2
	A	96.6	64.3	80.5	+6.3	112	9	51	23	2.1	-1.2
	S	75.4	47.6	61.5	-3.7	91	5	38	21	3.5	-0.6
	O	64.6	38.8	51.7	-1.4	85	4	13	29	5.8	-0.1
	N	49.3	31.5	40.4	+0.4	64	3	21	5	7.4	-0.1
	D	38.0	23.2	30.6	-2.0	50	21+	5	29	8.5	+0.4
1971		65.6	41.1	53.4	+0.3	112	Aug 9	5	Dec 29	5.9	+0.4
1972	J	39.2	21.8	30.5	+1.1	59	20	-4	28	7.8	
	F	44.0	25.7	34.8	-2.6	68	27	-1	3	8.2	
	M	59.5	34.4	47.0	+2.8	76	16-17	24	25	7.5	
	A	7.8	2.7	49.6	-2.9	78	27	26	3	6.3	

Table 3 shows the solar radiation and wind activity over the test period. Departure from the average solar radiation is on the high side with winds near normal except for peak gusts.

Table 3. SOLAR RADIATION AND WIND ACTIVITY

February 1971 to April 1972

		SOLAR RADIATION (LANGLEYS)						WIND (mph)		PEAK GUST		
	Month	Average Daily Total	Departure	Greatest Daily Total	Date	Least Daily Total	Date	Average Speed	Departure	Max. Min. Speed	Direction	Date
1971	J	114	-4	239	31	16	[illegible]	8.0	+1.7	59	WSW	9
	F	211	+11	329	28	54	9	8.6	+1.6	65	SW	24
	M	325	-15	514	31	82	10	8.9	+0.5	62	SSW	26
	A	488	+18	681	26	153	24	8.4	-0.6	50	WSW	11
	M	589	+18	755	28	156	31	10.1	+1.3	54	SSW	12
	J	619	-7	821	14	220	3	8.4	-0.8	39	WSW	13
	J	686	+27	802	2	253	9	8.3	-0.3	36	NW	4
	A	602	+51	703	3	242	22	7.8	-0.2	37	SW	30
	S	448	+30	573	4	121	28	8.0	+0.5	40	NNE	19+
	O	286	+24	430	1	58	30	7.2	+0.5	41	SSW	19
	N	148	+13	295	1	44	26	5.4	-0.8	44	SW	4
	D	96	+5	185	7	37	2	6.8	+0.8	45	SSW	13
1971		385	+171	821	June 14	16	Jan 16	8.0	+0.4	65	SW	Feb 24
1972	J	134	+16	249	29	50	20	10.3	+4.0	80	SW	11
	F	207	+7	368	29	76	18	7.3	+0.3	64	SW	27
	M	343	+3	536	26-29	47	1	7.5	-0.9	61	SW	5
	A	528	+58	704	28	300	5	11.1	+2.1	73	SSW	5

REFERENCE NOTES: +Also on earlier dates: [1]Sunrise to sunset. [2]Calories/sq. cm. [3]Visibility six miles or less.

INSTRUMENTED CABLE INSTALLATION

ASSEMBLY OF THE INSTRUMENTED CABLE

A porous cup type soil thermocouple psychrometer (TCP) was soldered to a shielded Beldon cable #8640 (two conductor #26 solid copper, color-coded vinyl jacket). The diode temperature transducer (DTT) was soldered to a Beldon coaxial cable (RG 174-U type, 50 ohms, 26 AWG strands). All TCP and DTT cables were bundled and taped together into one string with a stainless steel cable 1/6 inch in diameter. The stainless steel cable carried the entire cable weight during installation. The positions of the individual sensors on the cable are shown in Table 4.

Table 4. SOIL MOISTURE (PSYCHROMETER) AND TEMPERATURE PROBE INSTALLATION

Depth (in. or ft.)	Active Temperature Thermocouple	Active Moisture Psychrometer	Depth (ft.)	Active Temperature Thermocouple	Active Moisture Psychrometer
3"	Yes	Yes	40'	Not Working	Yes
6"	Yes	Yes	45'	Not Working	Not Working
9"	Yes	Yes	50'	Not Working	Yes
			55'	Yes	Not Working
1'	Yes	Yes	60'	Yes	Yes
1-1/2'	Yes	Yes	65'	Not Working	Not Working
2'	Yes	Yes	70'	Not Working	Yes
2-1/2'	Yes	Yes	80'	Yes	Yes
3'	Yes	Yes	90'	Yes	Yes
3-1/2'	Yes		100'	Yes	Yes
4'	Yes	Yes	110'	Yes	Not Working
4-1/2'	Yes	Yes	120'	Yes	Yes
5'	Yes	Yes	130'	Yes	Yes
5-1/2'	Yes	Yes	140'	Yes	Yes
6'	Yes	Yes	150'	Yes	Yes
7'	Yes	Yes	160'	Yes	Yes
8'	Yes	Yes	170'	Yes	Yes
9'	Yes	Yes	180'	Yes	Yes
10'	Yes	Yes	190'	Yes	Yes
11'	Yes	Yes	200'	Yes	Yes
12'	Yes	Yes	210'	Yes	Yes
13'	Yes	Yes	220'	Yes	Yes
14'	Yes	Yes	230'	Yes	Yes
15'	Yes	Yes	240'	Yes	Yes
17-1/2'	Yes	Yes	250'	Yes	Yes
20'	Yes	Yes	260'	Yes	Yes
22-1/2'	Yes	Yes	270'	Not Working	Yes
25'	Yes	Yes	280'	Yes	Yes
27-1/2'	Yes	Yes	290'	Yes	Yes
30'	Yes	Yes	300'	Yes	Yes
32-1/2'	Yes	Yes	310'	Yes	Yes
35'	Yes	Yes			

INSTALLATION OF THE INSTRUMENTED CABLE

The predominant vegetative cover in the vicinity of the well site is sagebrush (*Artemisia tridentata*) and cheatgrass (*Bromus tectorum L*). The soil is a relatively uniform sand to loamy sand containing a small amount of gravel throughout the soil profile with the water table approximately 310 feet below the surface.

The well was drilled using a dry core barrel. Stagger casing was used, as shown in Figure 1, to reduce skin friction between the casing wall and soil so that it would be possible to remove the casing. The soil material removed during the drilling process was labeled as to depth, stored in PVC bags, and sealed in metal cans to prevent the loss of soil water.

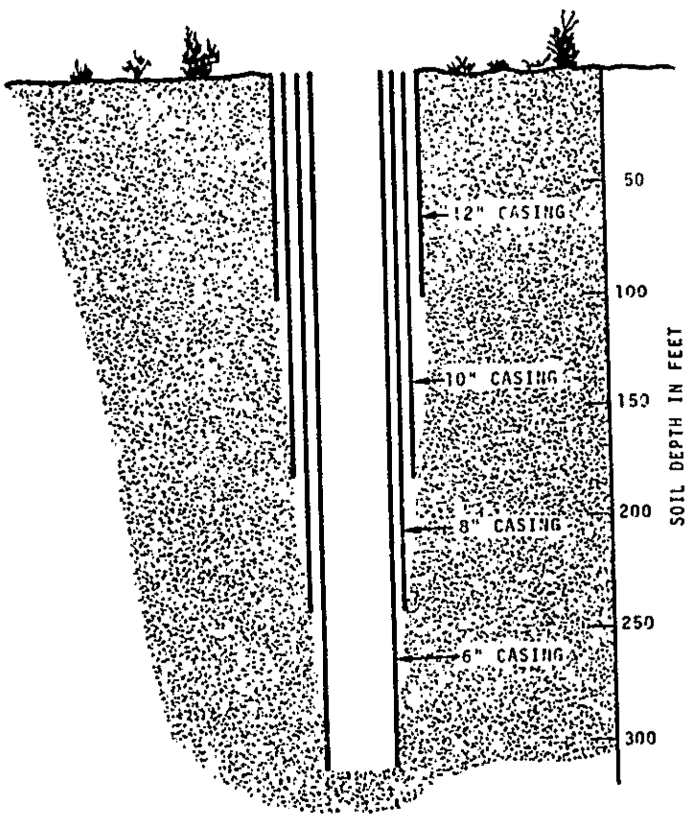

FIGURE 1. Stagger Well Casing Method

To protect the instruments during the backfilling process a PVC pipe was first lowered into the hole, and the instrumented cable, with soil thermocouple psychrometers and diode temperature transducers, was lowered inside the plastic pipe. As the well was backfilled the plastic pipe and well casing were gradually removed, leaving the instruments in place. The hole was carefully backfilled with the material previously removed. Satisfactory backfilling is a tedious and difficult process and additional work is required to improve the technique.

DATA ANALYSIS

Table 4 summarized ins ıt locations and operational status at the time the psychrome:ers and temperature probes were placed in the soil profile. Several instruments were lost between the 40 and 70 foot levels when the clasp holding the instruments was caught during removal of the casing. Future installations of this type will use a different holding method to eliminate the possibility of severing instruments in this manner.

Table 5 gives the soil composition at depths along the soil profile. The transducers were read periodically to determine when the soil reached equilibrium with the undisturbed soil. Figure 2 shows a nearly stable temperature profile. The temperature transducers were calibrated on an absolute scale to ±0.5°C and had a sensitivity of ±0.1°C. This temperature precision is more than adequate for use in temperature correction of the psychrometric measurements. Future installations should use a more rugged cable on the temperature transducers to reduce their loss.

Water content measurements were made on the soil samples taken throughout the soil profile during the drilling of the well. Figure 3 shows a plot of these data.

Figure 4 shows sets of the matric potential readings taken to observe the rate of stabilization. The data presented in this figure should not be used to evaluate water movement since the system has not stabilized. Figure 5 shows the time rate of stabilization of two thermocouple psychrometers. From these data it was projected that 90 percent of equilibrium will be reached in 200 to 250 days after installation.

Table 5. SOIL SEPARATES FOR PROFILE AT INSTRUMENT INSTALLATION

Depth Meters	Depth Feet	% Sand	% Silt	% Clay
1.5	5	95.1	3.3	1.6
3.0	10	98.6	0.2	1.6
4.6	15	92.3	4.6	3.1
6.1	20	81.9	16.7	1.4
7.6	25	89.2	9.4	1.4
9.2	30	90.2	8.4	1.4
10.7	35	90.7	7.9	1.4
12.2	40	90.9	6.7	2.4
13.7	45	83.7	12.8	3.5
15.3	50	78.9	18.6	2.5
16.8	55	90.6	6.9	2.5
18.3	60	67.6	28.4	4.0
19.8	65	83.6	12.9	3.5
20.4	70	82.4	13.8	3.8
23.9	75	73.8	21.2	5.0
24.4	80	93.7	4.7	1.6
26.0	85	84.4	12.8	2.8
27.5	90	92.9	5.3	1.8
29.0	95	94.2	12.0	3.8
30.5	100	89.5	8.7	1.8
32.1	105	86.4	10.7	2.9
33.6	110	90.5	7.6	1.9
35.1	115	84.7	12.0	3.3
36.6	120	91.2	7.0	1.8
38.1	125	85.6	11.7	2.7
39.6	130	90.9	6.8	2.3
41.2	135	83.9	13.9	2.3
42.7	140	80.0	15.6	4.4
44.2	145	84.9	12.6	2.5
46.8	150	89.3	8.5	2.2
47.3	155	84.3	13.0	2.7
48.8	160	84.5	12.8	2.7
50.3	165	89.6	8.2	2.2
51.8	170	89.0	8.8	2.2
53.4	175	85.0	12.5	2.5
54.9	180	84.8	12.5	2.7
56.4	185	86.8	10.3	2.9
58.0	190	92.8	5.7	1.5
59.5	195	90.0	7.5	2.5
61.0	200	91.9	6.7	1.4
62.5	205	80.4	14.7	4.9
64.0	210	61.8	33.1	5.1
65.6	215	81.8	14.3	3.9
67.1	220	86.0	12.5	1.5
68.6	225	85.5	11.0	3.5
70.2	230	89.5	9.1	1.4
71.7	235	55.9	35.9	8.2
73.2	240	92.9	5.4	1.7

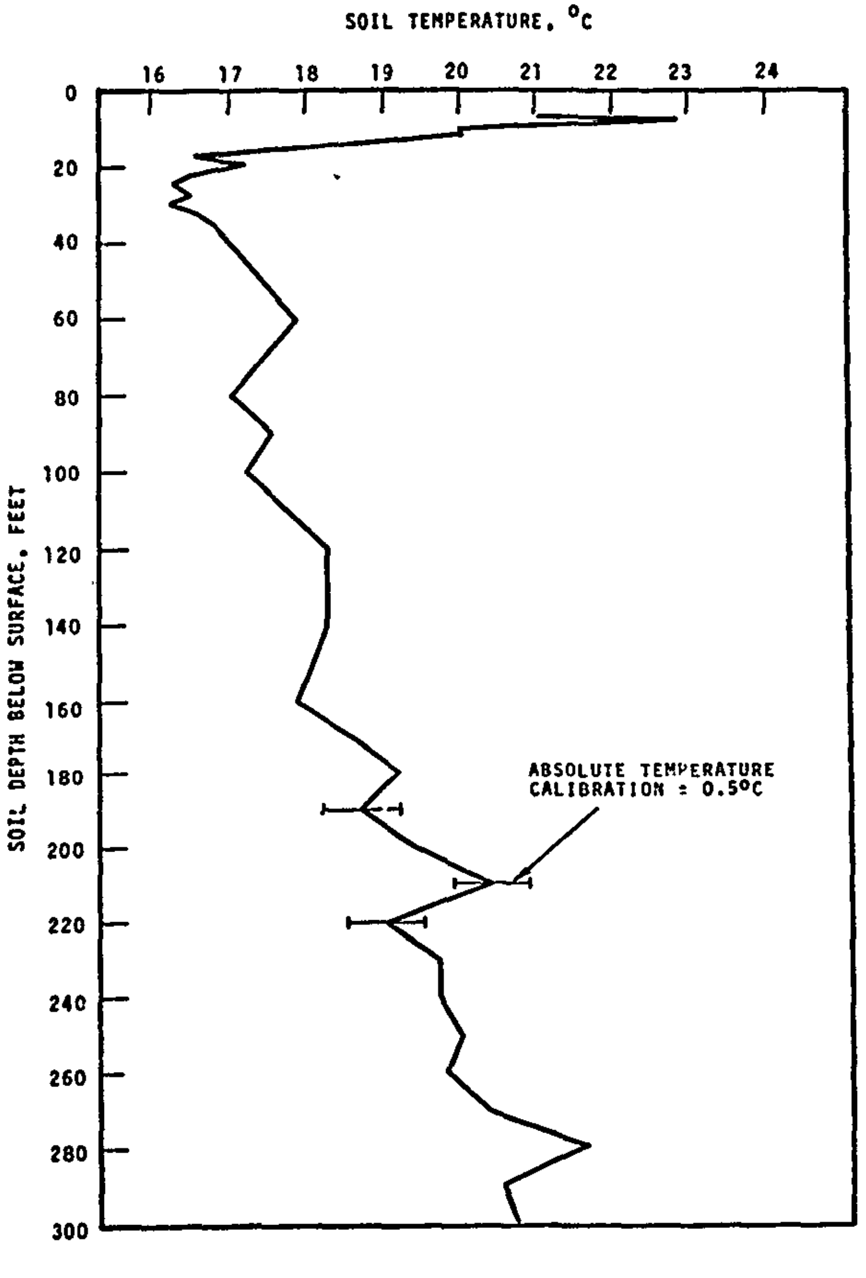

FIGURE 2. Soil Temperature Profile October 13, 1970

9 3 1 2 8 7 2 1 3 2 7

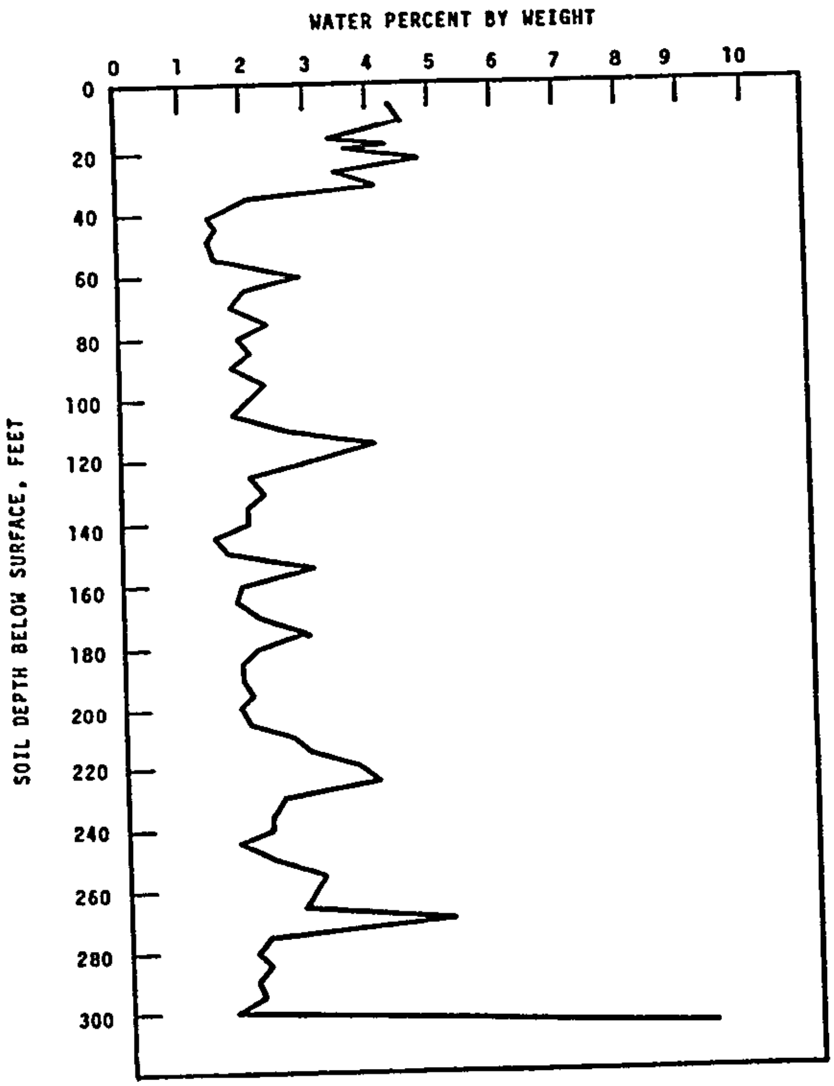

FIGURE 3. Water Content by Weight of Original Soil Profile

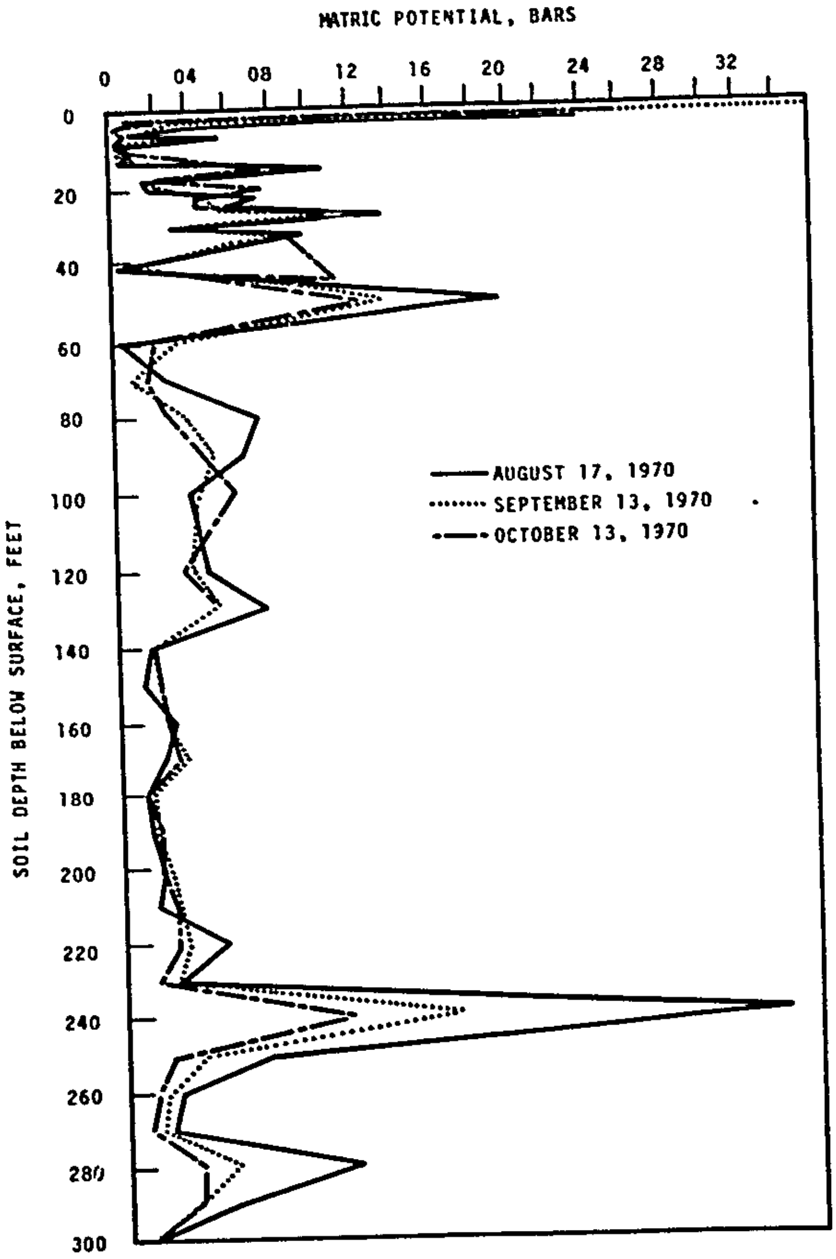

FIGURE 4. Water Potential as a Function of Soil Depth

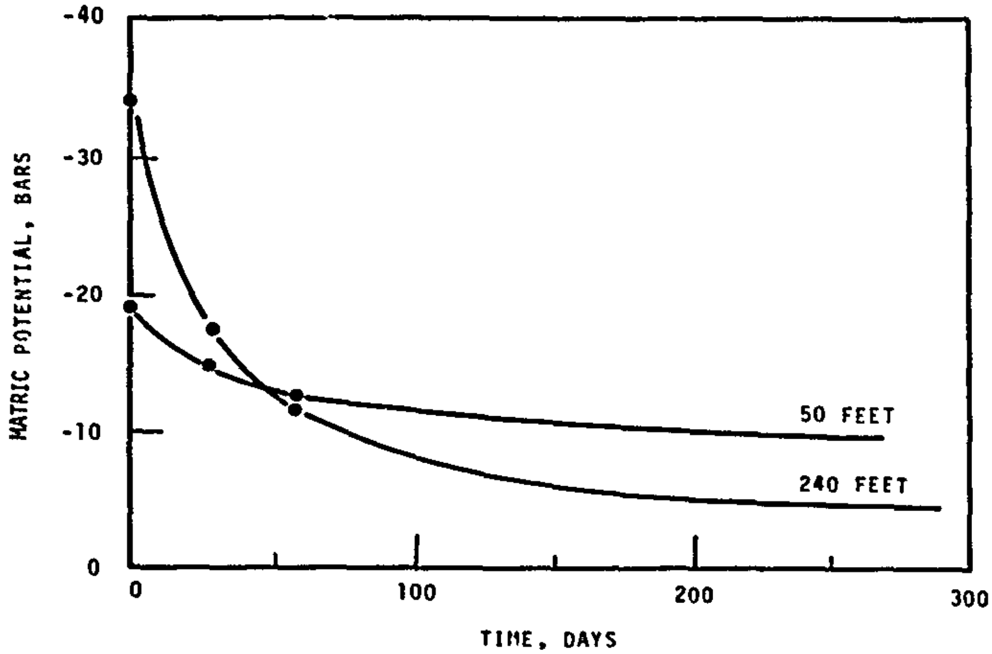

FIGURE 5. Projected Equilibrium Curve for the Soil Psychrometers at 50 and 240 Feet

SOIL MOISTURE TREND ANALYSIS

The psychrometer data from February 1971 to May 1972 were averaged for each month and plotted by depth. A typical plot of matric potential in bars plotted against depth in feet is shown in Figure 6. In order to separate the curves, time-spaced months were selected for plotting together. The complete set of graphs of these data are shown in Appendix B. The rugged curve reflects the water content in the original profile. The highly fluctuating values in the curves seem to be real since similar results were obtained by different means as described below.

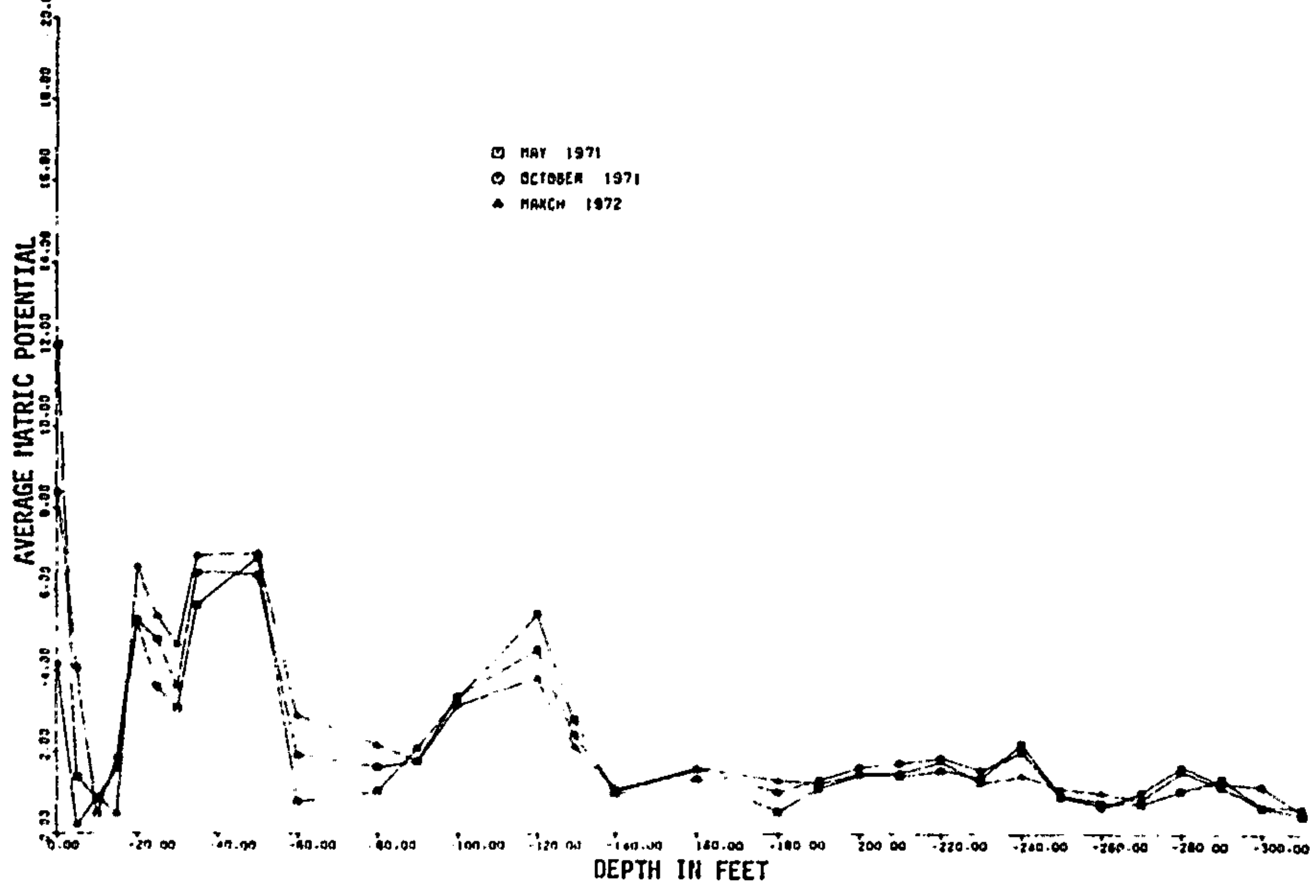

FIGURE 6. Matric Potential Versus Depth for Selected Month

The matric potential in a soil system is decreased by the attraction of solutes to the soil particles (adsorption forces). For a nonsaline soil such as that under study the capillary potential is the major component of the matric potential in an isothermal condition. The soil water matric potential curve was derived from the desorption curves using a pressure-membrane and pressure-plate apparatus for a series of soil samples obtained at various depths from Well 699-19-47B, located 6 miles southeast of the 200 East Area. The matric potential profile (Figure 7) was obtained by referring the field moisture contents of the soil samples to their corresponding desorption curves, assuming the osmotic, temperature, and hysteresis effects to be negligible. The general shape of this matric water potential profile was very similar to the matric potential profile obtained from the soil psychrometers. The lowest matric potential (driest region) occurred at about 45 feet beneath the ground surface.

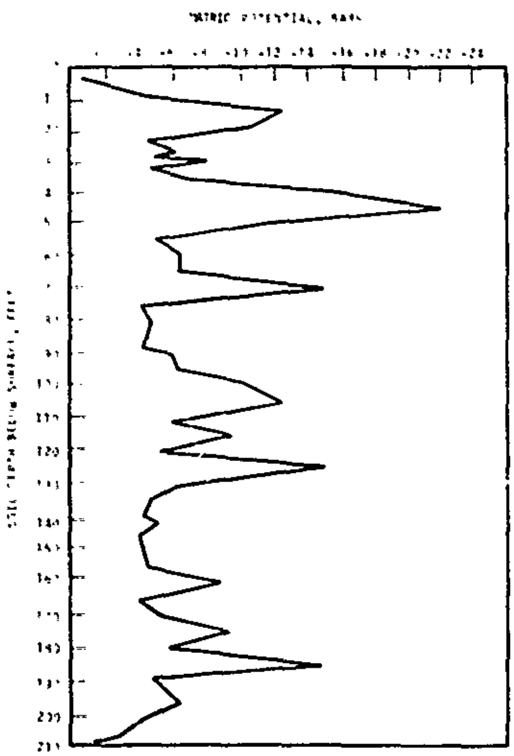

FIGURE 7. Soil Water Matric Potential as a Function of Depth in Well 699-19-47B

A time-based trend analysis for these data required that data for each psychrometer depth be plotted as a function of time. To obtain less erratic data only the monthly averaged readings were plotted. Figure 8 is a typical plot of the average matric potential as a function of time. Fifteen months of data are plotted from 0 to 14, starting with February 1971, in Figures C-1 through C-17. The widely spaced depths on the graph are used to separate the curves on the plots.

The matric potentials in the upper soil profile show a yearly cycle. The matric potential at the surface is influenced strongly by weather conditions such as precipitation, evapotranspiration, and temperature. For example, the 0.25 foot depth has the greatest negative matric potential for the month of August which corresponds to the maximum air temperatures. For the lower soil depths the negative maximum is less and shows a time lag. Somewhere below the 12 foot depth the yearly cycle vanishes.

To determine trends in the soil moisture content a best fit straight line was visually drawn through the mean monthly water potentials. The matric potentials for February 1971 and April 1972, as determined from the best fit line, were used as the initial and final values, respectively, in the trend analysis. The ratio of these two values was used to determine trends in the soil moisture content. Arbitrarily it was assumed that no significant change occurred for ratios between 0.75 and 1.25. The results are summarized in Table 6. Of the 34 soil depths studied, the moisture content is considered unchanged at 15 depths, drier at 14 depths, and wetter at only 4 depths indicating that the water potential of the soil profile as a whole did not change very much. If there is any significant trend at all, it is a slight drying of the soil. The driest region is between 20 feet and 60 feet.

TEMPERATURE MEASUREMENTS

Simultaneously with the psychrometer readings, temperature measurements were made and recorded from the temperature transducers. These data are necessary for determining the temperature gradient and its effect on soil moisture.

Figure 9 is a typical plot showing the averaged monthly temperature profile over the depth in feet; Figures D-1 through D-5 show additional profiles. The seasonal cycling is seen by the whip-like action of the curve above 20 feet. Below this level the variation in the curve seems to be due to instrument noise variation. Even with this noise, the earth's thermal gradient is easily identified.

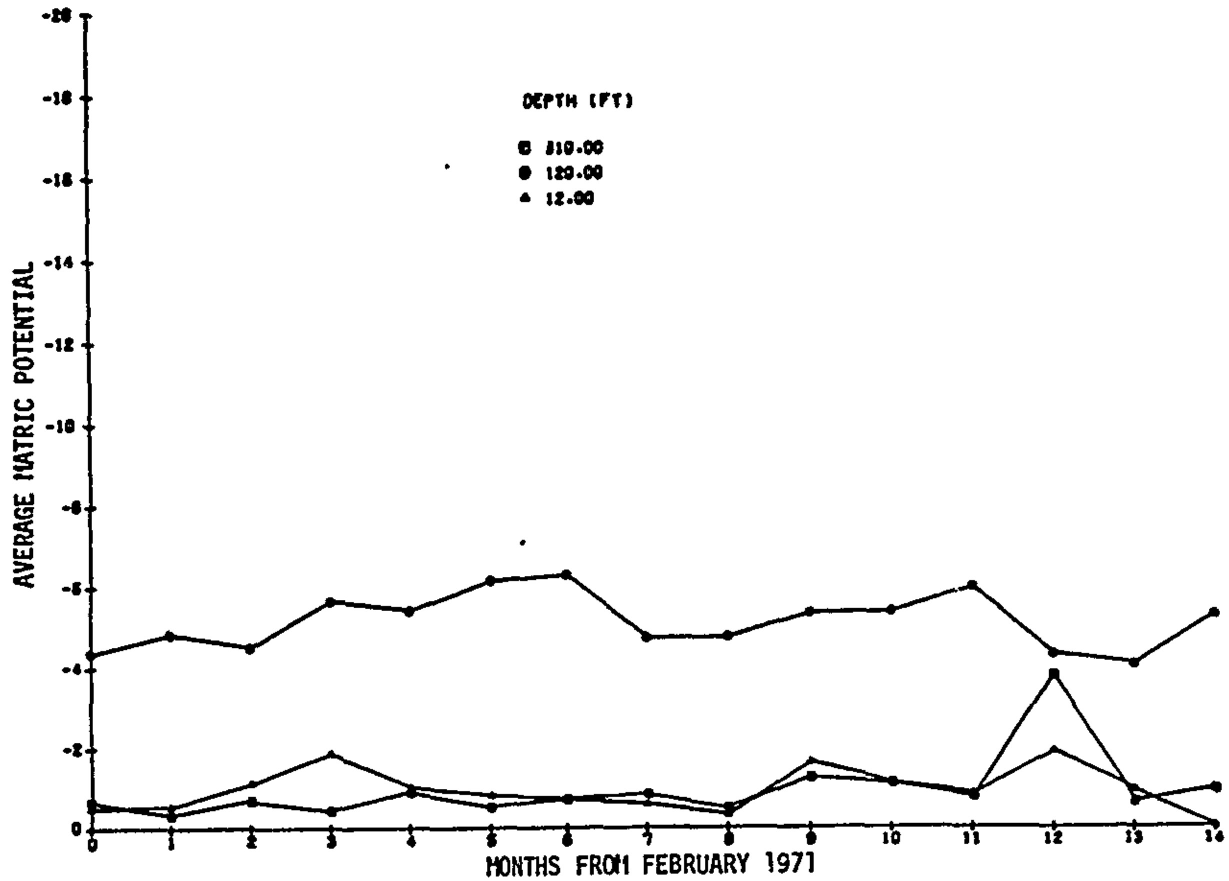

FIGURE 8. Average Monthly Matric Potential Versus Time for Selected Psychrometer Depths

Table 6. THE TREND OF MATRIC POTENTIAL VALUE. AT VARIOUS SOIL DEPTHS FROM THE SOIL SURFACE

Soil Depth Feet	Matric Potential Bars Initial	Final	Ratio	Unchanged	Matric Potential Trend to Become Drier	Wetter
13	0.8	0.9	0.9	0		
14	1.3	1.1	1.2	0		
15	2.2	0.6	3.7			+
17.5	0.8	0.8	1.0	0		
20	4.3	5.8	0.7		-	
22.5	2.4	2.4	1.0	0		
25	3.5	5.3	0.7		-	
27.5	6.7	6.8	1.0	0		
30	2.8	4.6	0.6		-	
32.5	5.9	6.4	0.9	0		
35	5.4	7.3	0.7		-	
50	7.3	6.5	1.1	0		
60	0.7	2.8	0.3		-	
80	0.9	1.9	0.5		-	
90	2.1	1.6	1.3			+
100	3.5	3.1	1.1	0		
120	4.8	4.9	1.0	0		
130	2.9	2.3	1.3			+
140	1.0	1.7	0.6		-	
160	1.2	1.9	0.6		-	
180	0.6	1.5	0.4		-	
190	1.3	1.5	0.9	0		
200	1.4	1.5	0.9	0		
210	1.7	1.6	1.1	0		
220	1.7	1.9	0.9	0		
230	1.5	1.4	1.1	0		
240	2.9	1.5	1.9			+
250	1.0	1.3	0.7		-	
260	0.8	1.1	0.7		-	
270	0.9	1.2	0.7		-	
280	1.2	1.7	0.7		-	
290	1.5	1.5	1.0	0		
300	0.7	?	?			
310	0.5	1.1	0.5		-	
TOTAL				15	14	4

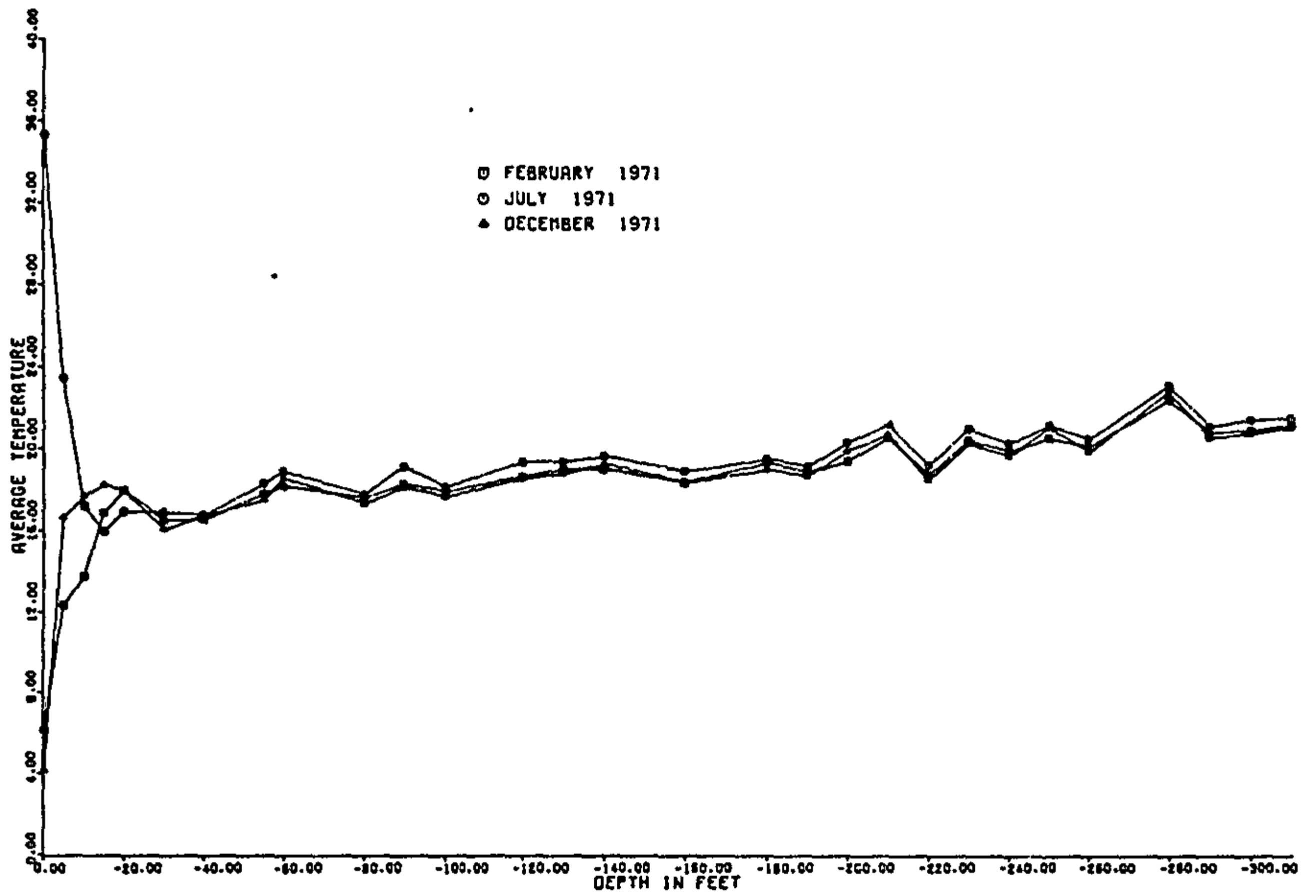

FIGURE 9. Average Measured Monthly Soil Temperature as a Function of Depth for Selected Month

Because of the difficulty of determining long-term trends, the data were replotted as average temperature versus the time for months from February 1971 to April 1972; these plots are shown in Figure 10 and in Figures D-6 through D-23. The seasonal cycling in the upper level curves and the time lag of thermal transfer is easily seen from these curves. Below the 20 foot level the curves show essentially no seasonal or long-term trends. Small seasonal rises in all curves of about 1°C have been attributed to the ambient temperature of the recording equipment.

CONCLUSIONS

In summary, the results to date do not permit a definite conclusion as to whether precipitation water will eventually reach the groundwater table. The matric potentials seem to indicate that the soil is becoming drier and that the water flux is extremely small. If any flow at all existed, this minute flow decreased further during the study period.

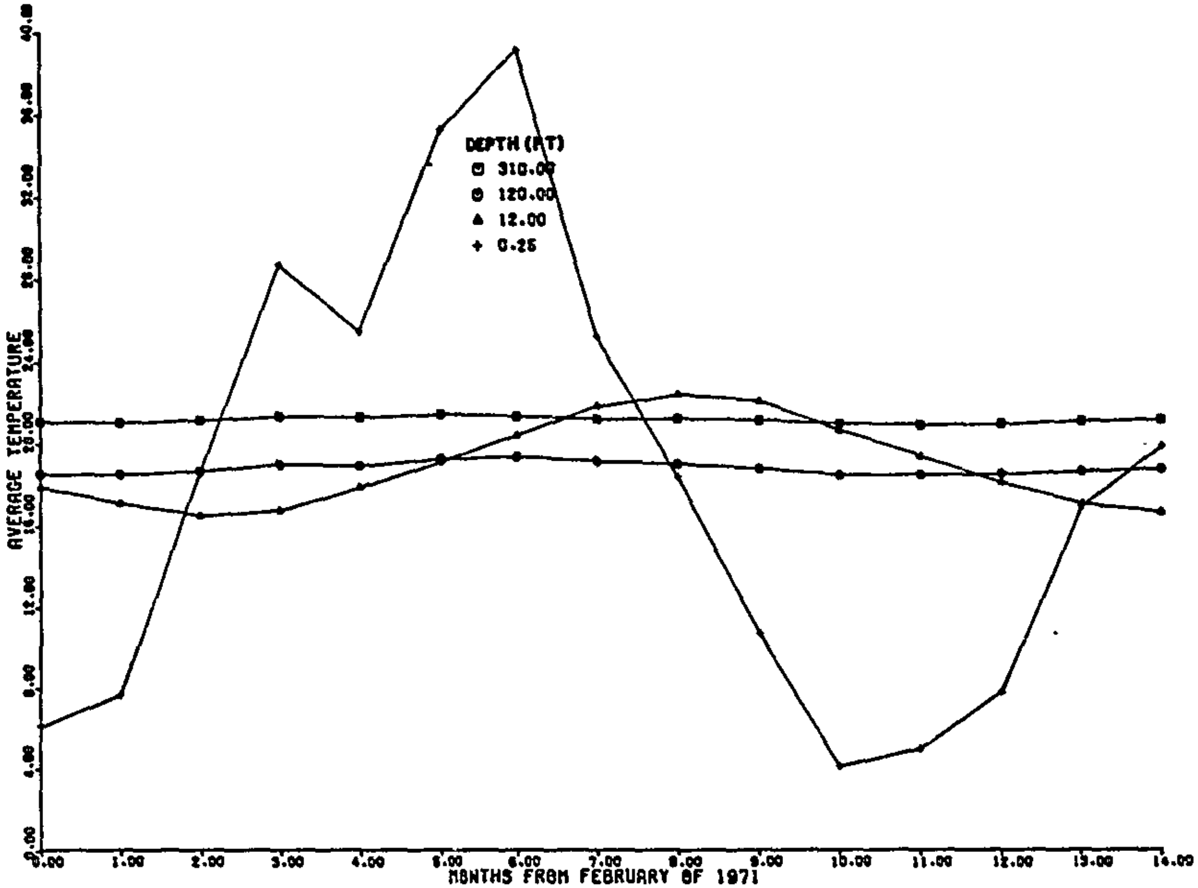

FIGURE 10. Average Measured Monthly Soil Temperature (°C) Versus Time for Selected Depths

ACKNOWLEDGMENTS

The authors would like to thank Harvey Huber for his assistance in constructing and installing the instruments and his faithful gathering of the data herein. Richard Buchanan reduced the voluminous data to computer plots.

This research was sponsored by the Advanced Technology Development Section, Research and Development Department, Atlantic Richfield Hanford Company. The authors are grateful for the assistance and direction provided D. J. Brown, Staff Geologist and R. E. Isaacson, Manager of the Advanced Technology Development Section of Atlantic Richfield Hanford Company.

APPENDIX A

BASIC SOIL-WATER RELATIONSHIPS

APPENDIX A

Soil water in a natural condition is dynamic. It is almost always moving from one location to another in response to driving forces created by infiltration, evaporation, rainfall, temperature, plant use, etc., and these driving forces are changing in space and time. When information concerning the movement of water in the soil is desired, it is best to describe the soil water in terms of soil moisture potential because the movement rate is strongly related to the change in energy of the mass moisture moved, i.e., water potential.

A standard terminology does not exist which is acceptable and meaningful to all workers in this field. Of the many available terms, water potential seems most satisfactory because it is consistent with the basic concepts of thermodynamics. Furthermore, the use of the word potential enables one to isolate and evaluate the various components such as the osmotic, capillary, and gravitational forces which affect the total potential of water in various parts of the system.

The Gibbs free energy of a system is an expression of the system's capacity to do work. This depends on the mean free energy of a particle as well as the concentration of particles (mole fraction) of the substance under consideration. The free energy of soil water in a given condition, with temperature and pressure held constant, can be expressed as a chemical potential.

The net potential of the water in a soil system (μ_w) is equal to the chemical potential of a pure, free water ($\mu_w°$) adjusted for the various effects of those forces in the system which change its chemical potential. If the effects of all these forces can be expressed through their influence on vapor pressure, then:

$$\mu_w = \mu_w° + RT \ln e/e°$$

or

$$\mu_w - \mu_w° = RT \ln e/e° \quad (1)$$

where

R = ideal gas constant (erg/mole/dyne)

T = the absolute temperature (°K)

e = vapor pressure of water in the system at temperature T

e° = the vapor pressure of pure, free water at the same temperature T.

The e/e° is the relative humidity and its value is less than one. Therefore, $\ln e/e^\circ$ is a negative number. The resulting net water potential is thus a negative number; i.e., the soil water potential energy is less than that of pure free water.

The unit of chemical energy is ergs/mole and it is convenient to convert to more familiar pressure units by dividing both sides of Equation 1 by the partial molal volume of water, V_w.

$$\frac{\mu_w - \mu_w^\circ}{V_w} = \frac{RT \ln e/e^\circ}{V_w}$$

$$= \frac{RT}{V_w} \ln e/e^\circ$$

$$= \psi_w = \text{water potential} \qquad (2)$$

Now:

$$\frac{\text{erg/mole}}{\text{cm}^3\text{/mole}} = \frac{\text{erg}}{\text{cm}^3} = \frac{\text{dyne x cm}}{\text{cm}^3} = \text{dyne/cm}^2$$

$$= \text{a unit of pressure}$$

and 1 bar = 0.987 atm. = 10^6 dyne/cm^2 or 10^6 erg/cm^3.

Equation 2 indicates that ψ_w is equivalent to the difference in free energy per unit molal volume of water between water in the system and pure free water.

Water potential is decreased by the addition of solutes, by the matric or capillary force which is the adhesive force originating from soil particles and their arrangements, by the negative ambient atmospheric pressure, and by gravity force. This relationship under isothermal conditions can be expressed as

$$\psi_{water} = \psi_s + \psi_p + \psi_m + \psi_g$$

where potential energies are due to solute (ψ_s), pressure (ψ_p), matric or capillary force (ψ_m), and gravity force (ψ_g), respectively.

In regard to the physical measurements of the above potential energies, soil psychrometers will measure ψ_s, ψ_p and ψ_m. The gravity force ψ_g can be readily determined by knowing the elevation with respect to a given reference (usually mean sea level). The difference between the pressure plate measurements (ψ_m) and the psychrometer measurements (ψ_s, ψ_p and ψ_m) provides a quantitative measure of the solute and pressure forces.

The above water potential (ψ_w) is for isothermal, bulk liquid flow. If the temperature distribution as determined by temperature transducers is known, the contribution of the nonisothermal component to the bulk liquid movement and of the vapor flux can be calculated.

APPENDIX B

MATRIC POTENTIAL VERSUS DEPTH PLOTTED FOR SELECTED MONTHS

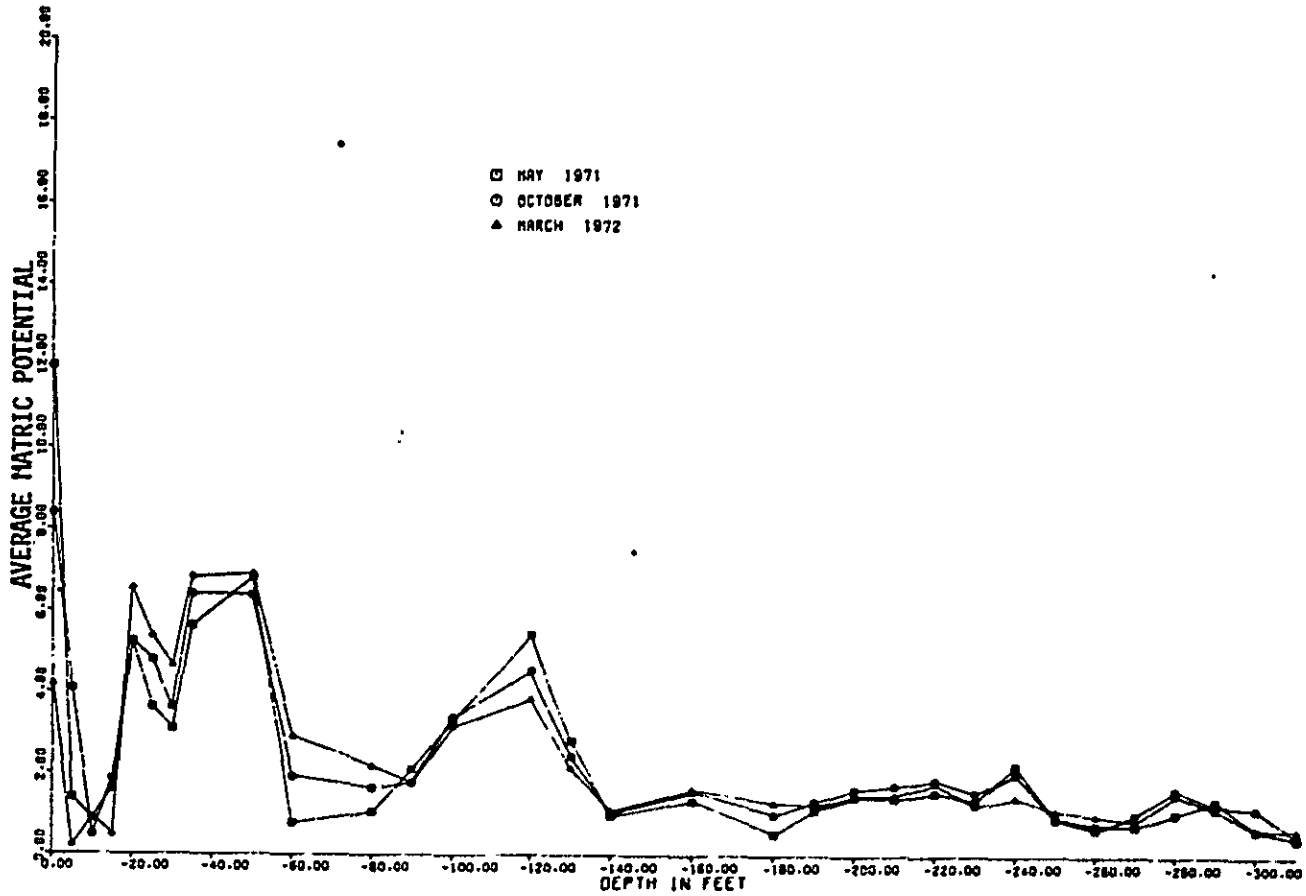

FIGURE B-1. Matric Potential Versus Depth for Selected Months

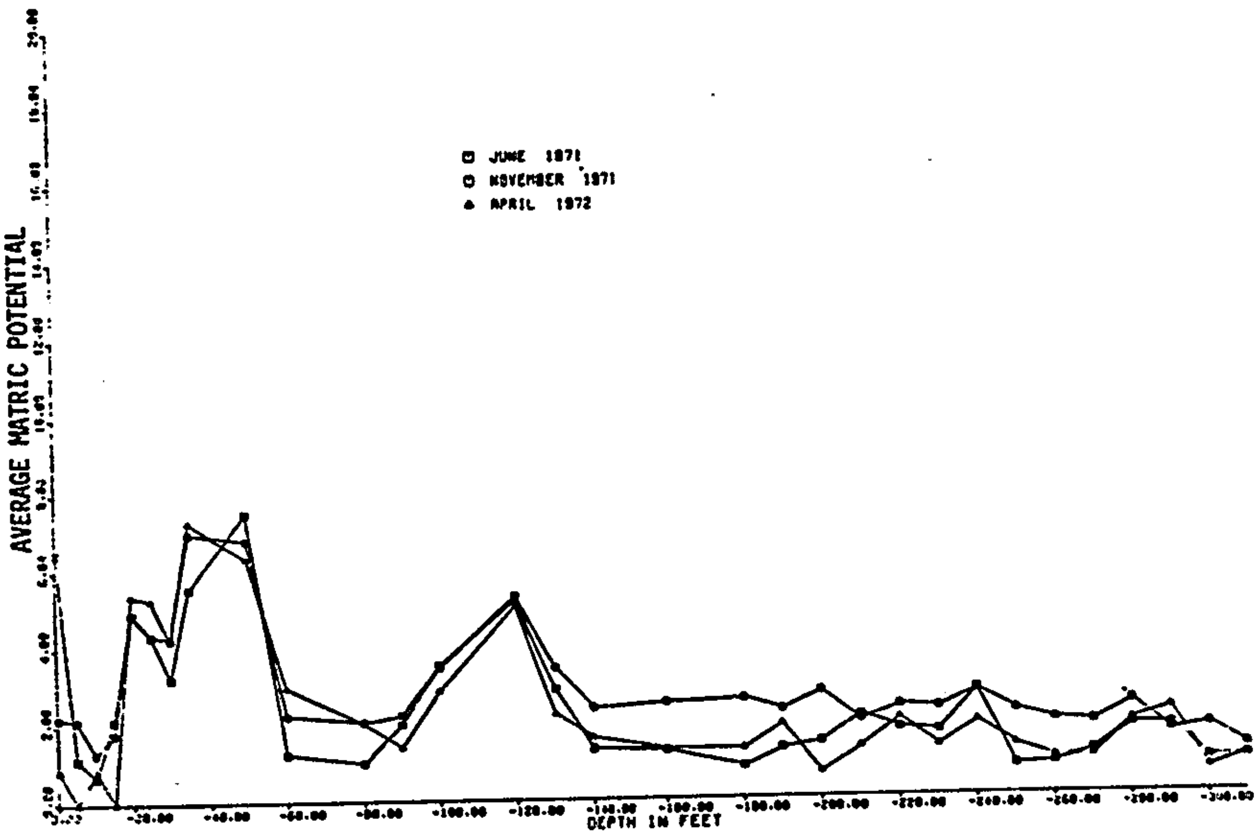

FIGURE B-2. Matric Potential Versus Depth for Selected Months

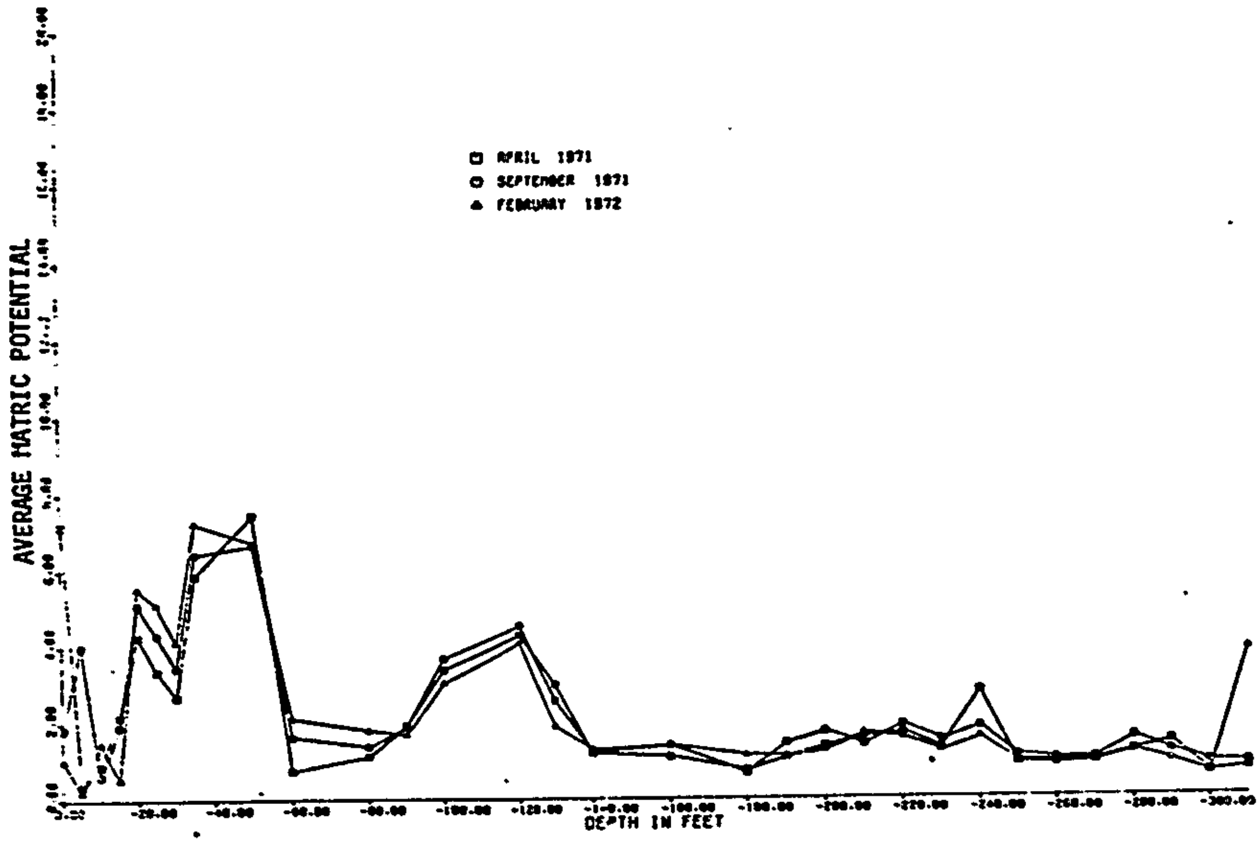

FIGURE B-3. Matric Potential Versus Depth for Selected Months

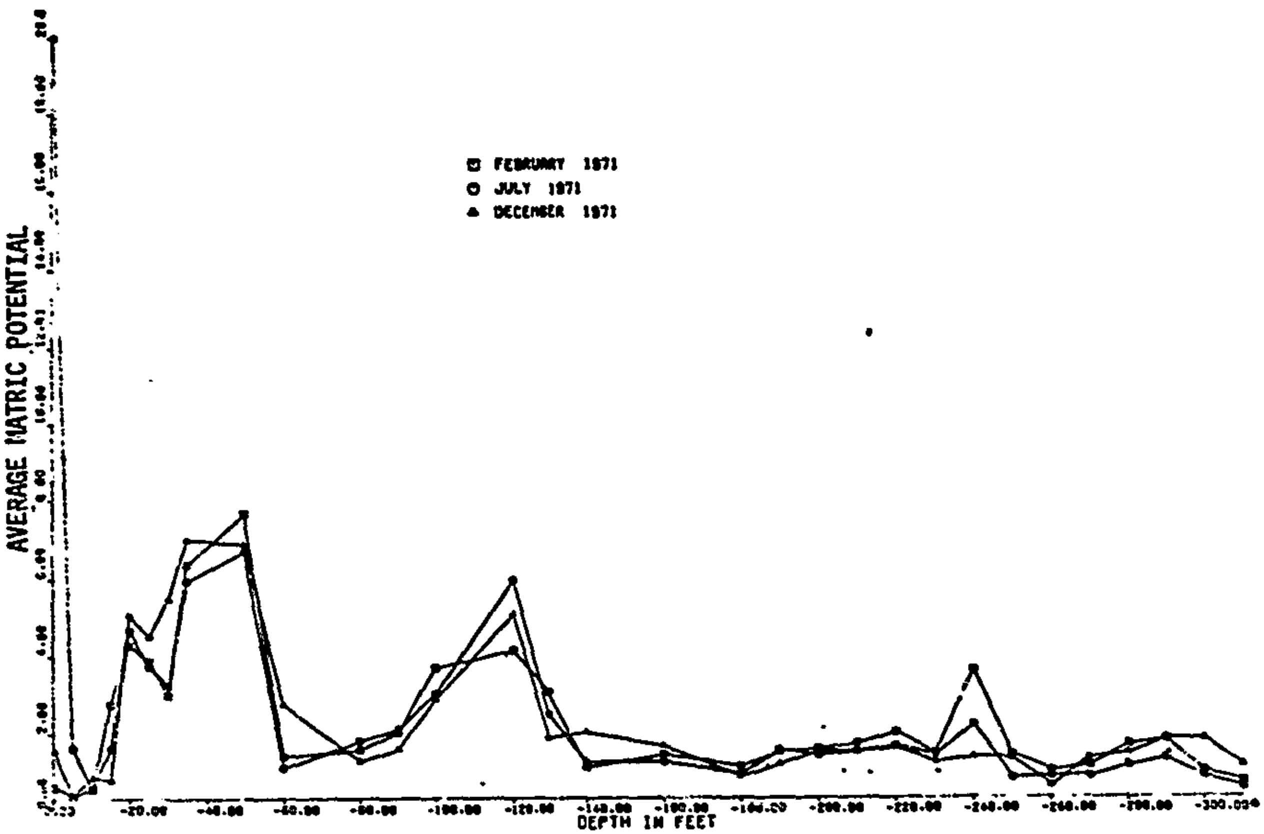

FIGURE B-4. Matric Potential Versus Depth for Selected Months

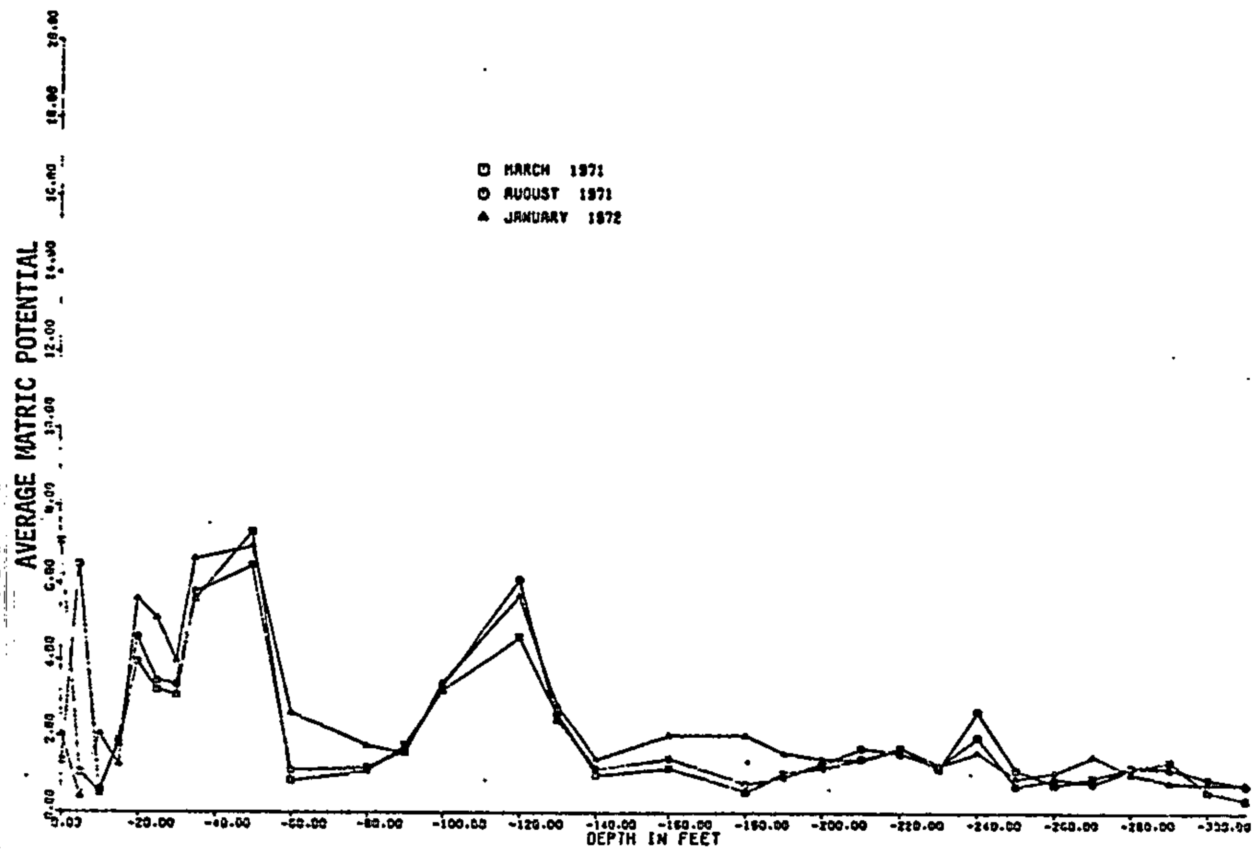

FIGURE B-5. Matric Potential Versus Depth for Selected Months

APPENDIX C

AVERAGE MONTHLY MATRIC POTENTIALS FOR SELECTED PSYCHROMETER DEPTHS

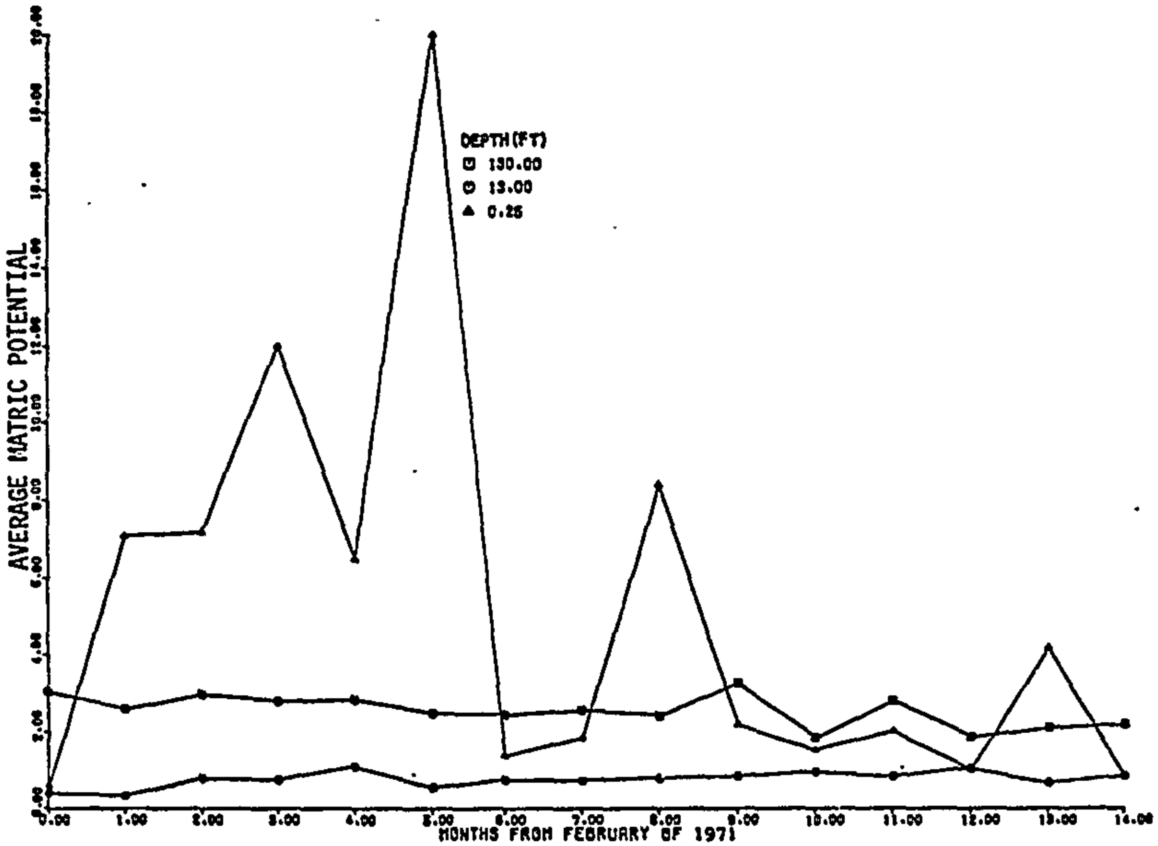

FIGURE C-1. Average Monthly Matric Potential Versus Time for Selected Psychrometer Depths

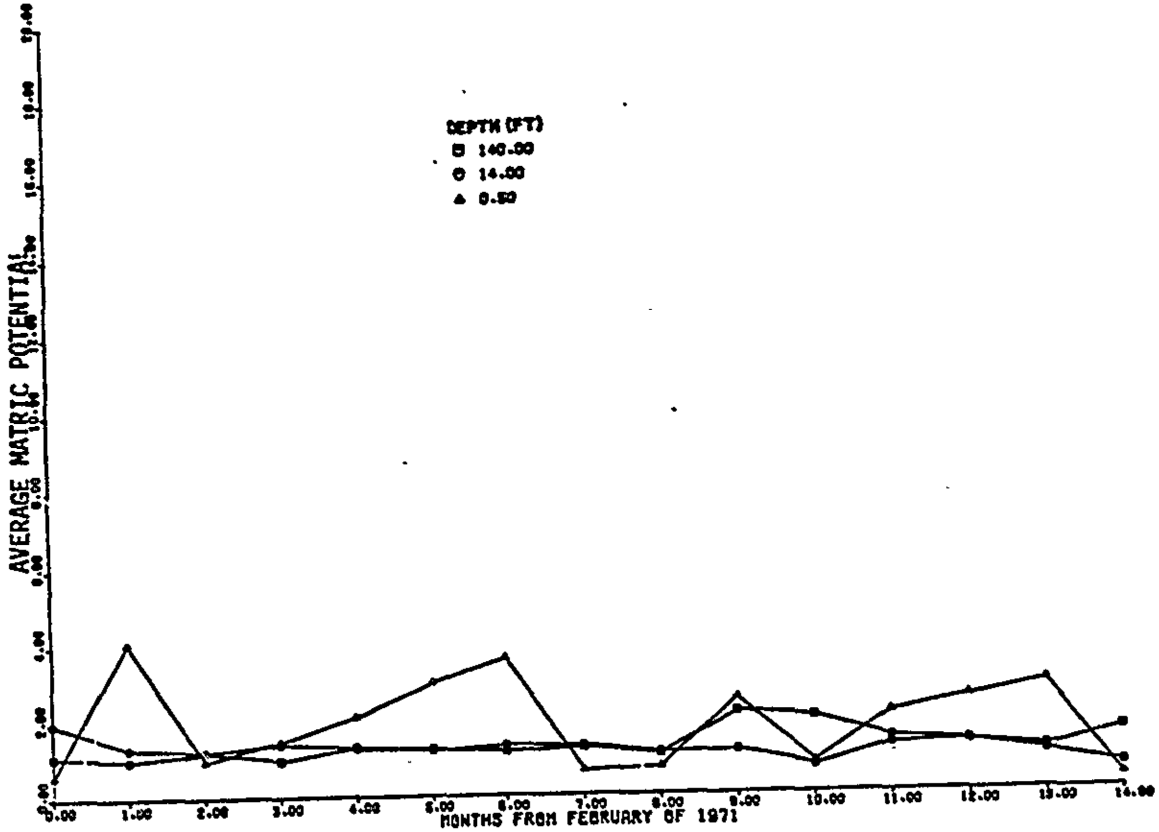

FIGURE C-2. Average Monthly Matric Potential Versus Time for Selected Psychrometer Depths

9 3 1 2 8 7 2 0 3 5 3

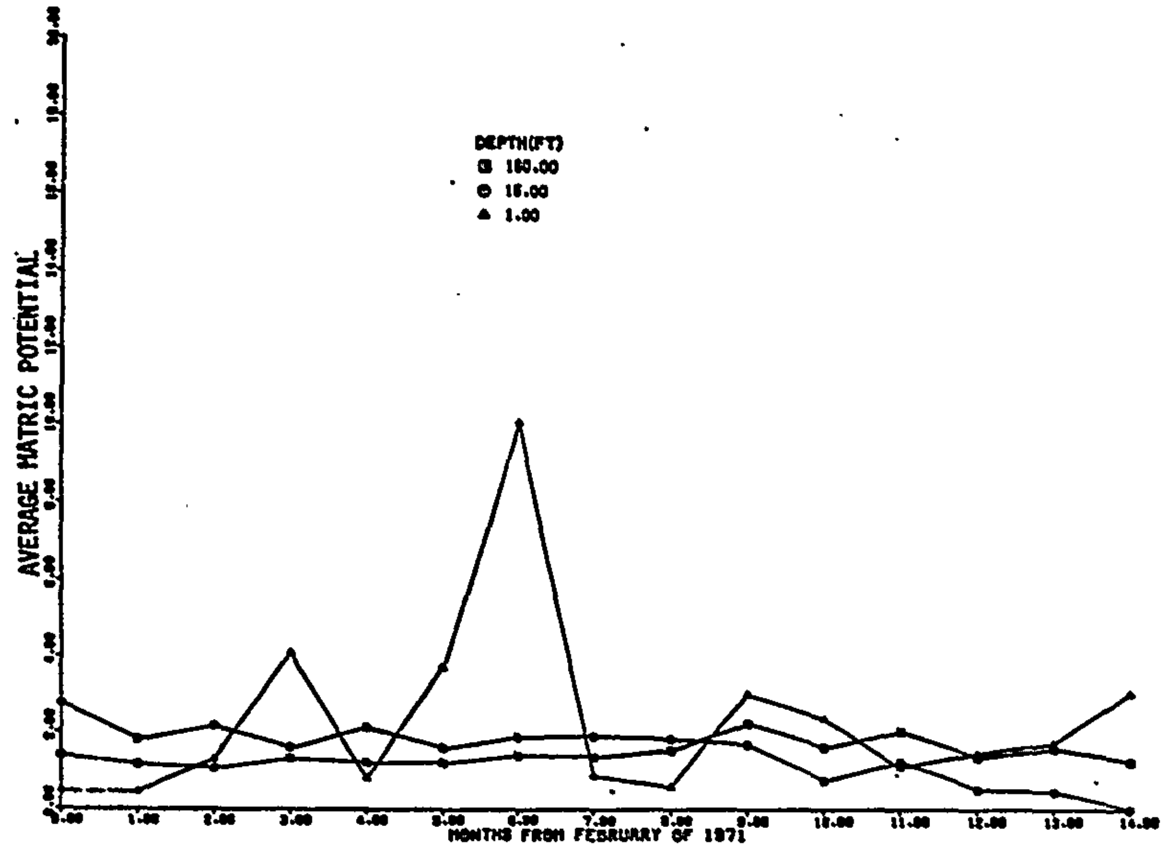

FIGURE C-3. Average Monthly Matric Potential Versus Time for Selected Psychrometer Depths

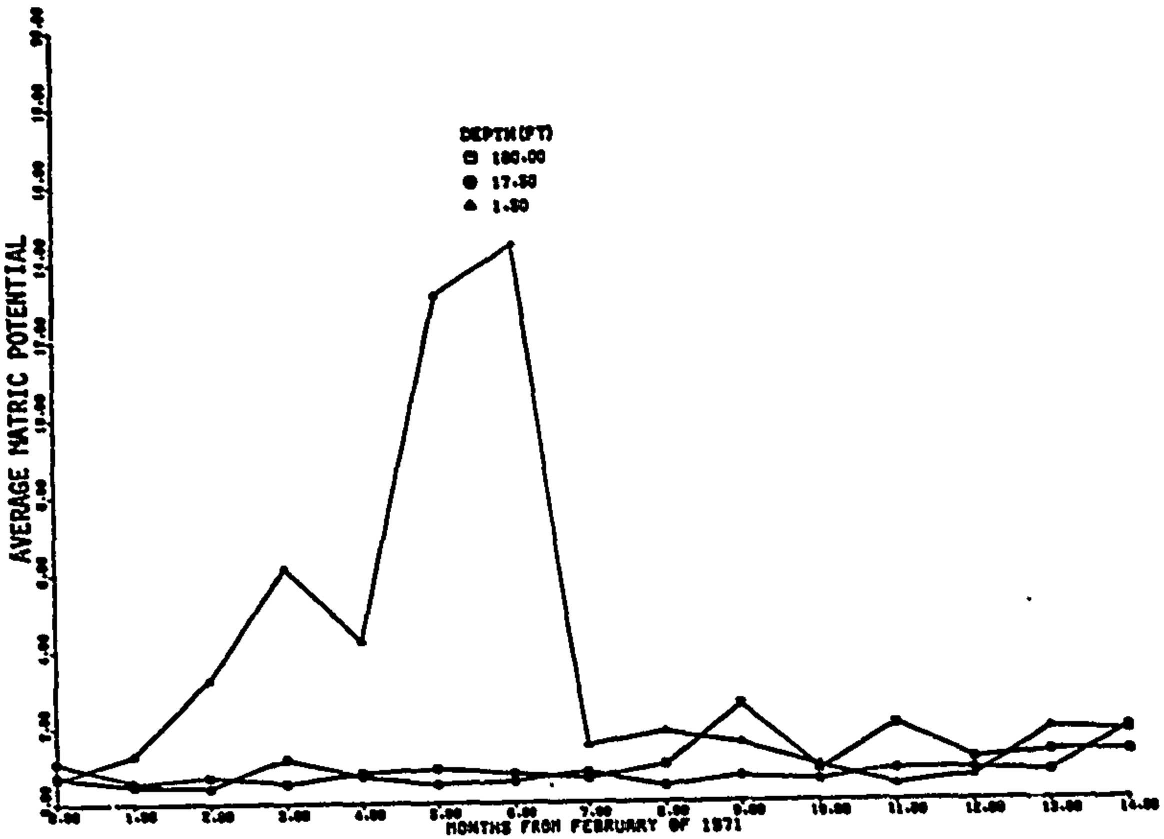

FIGURE C-4. Average Monthly Matric Potential Versus Time for Selected Psychrometer Depths

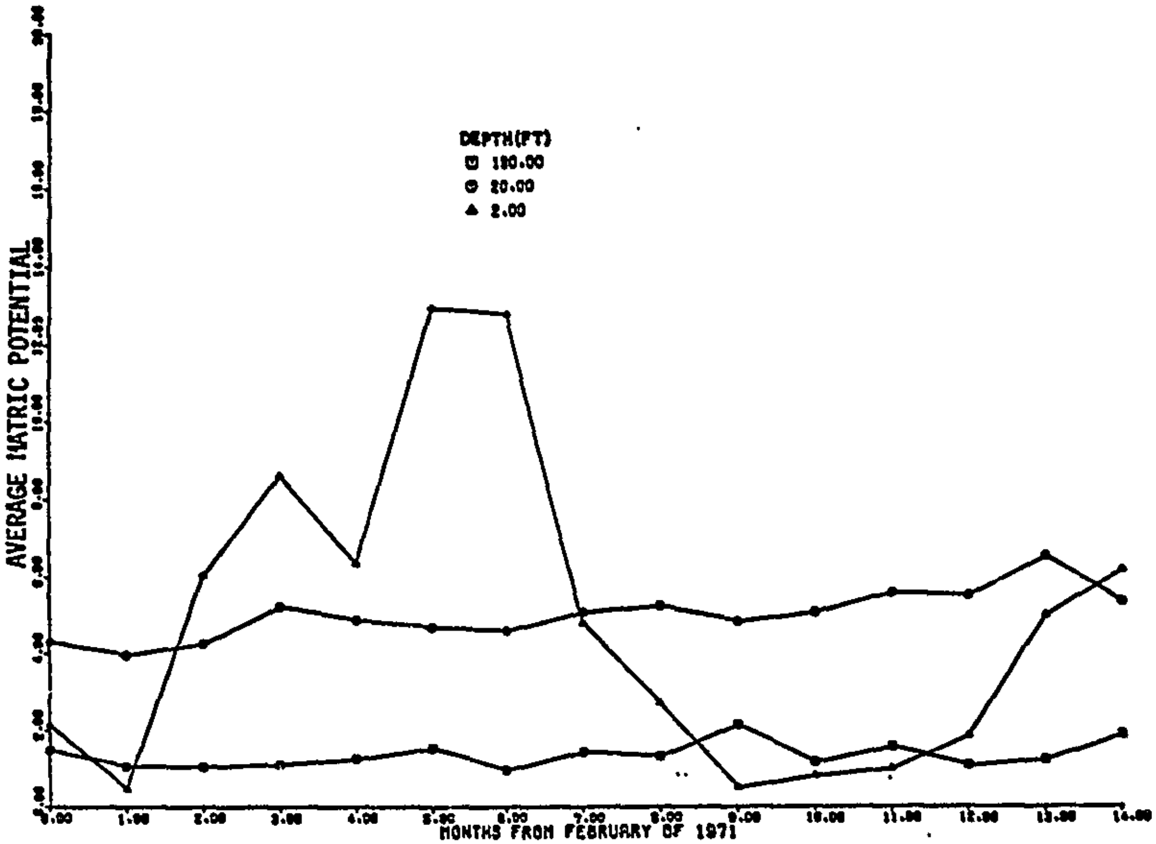

FIGURE C-5. Average Monthly Matric Potential Versus Time for Selected Psychrometer Depths

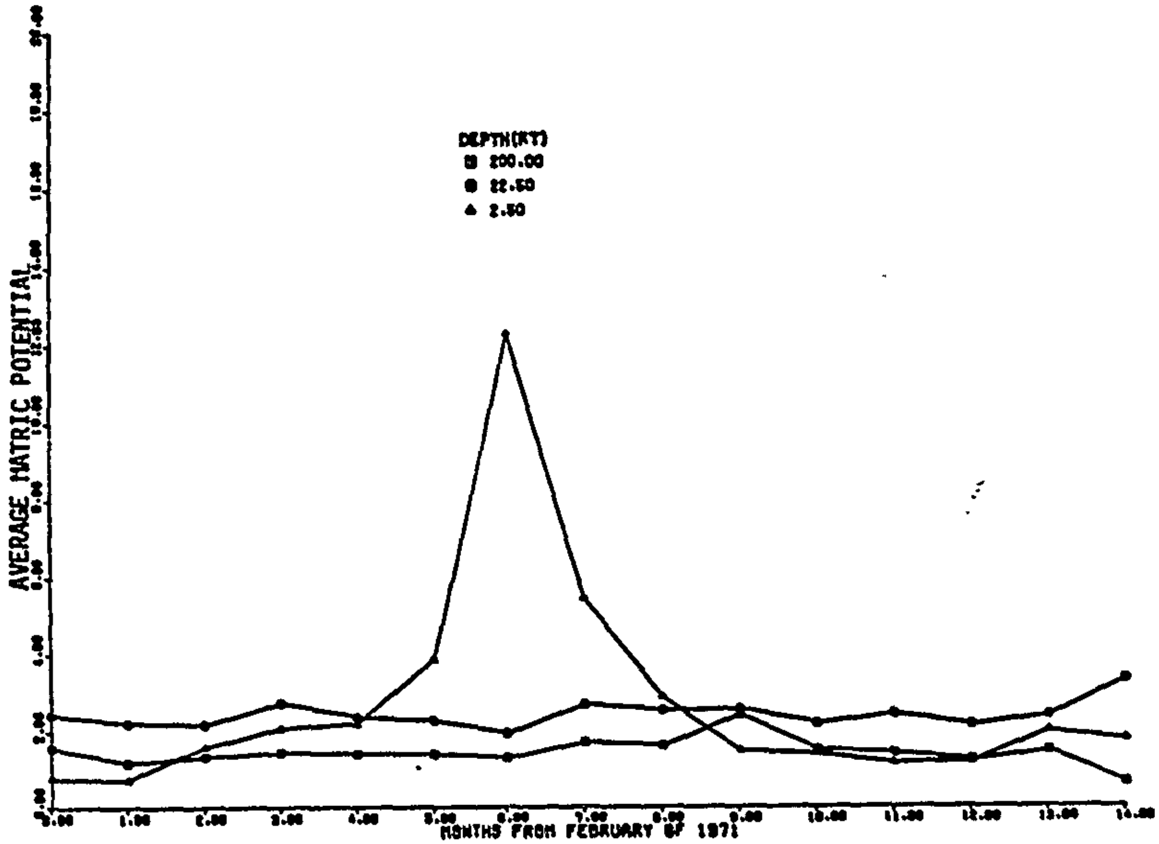

FIGURE C-6. Average Monthly Matric Potential Versus Time for Selected Psychrometer Depths

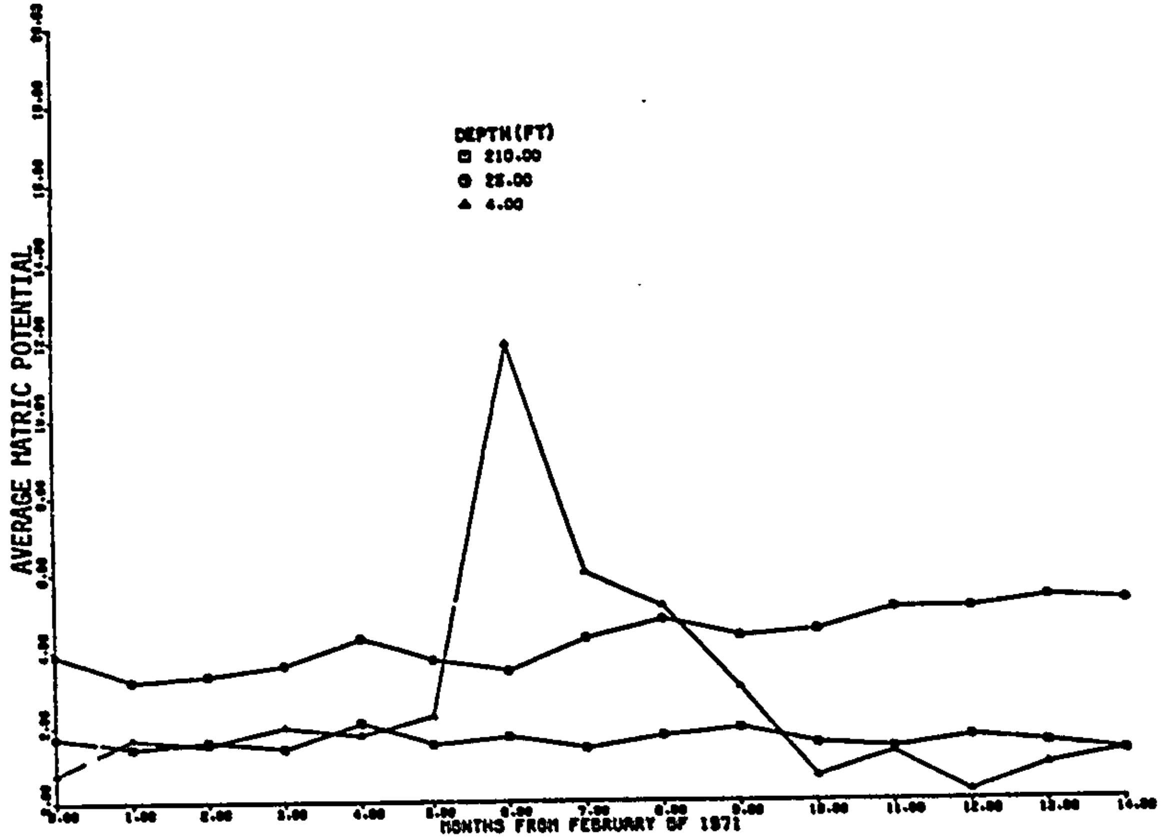

FIGURE C-7. Average Monthly Matric Potential Versus Time for Selected Psychrometer Depths

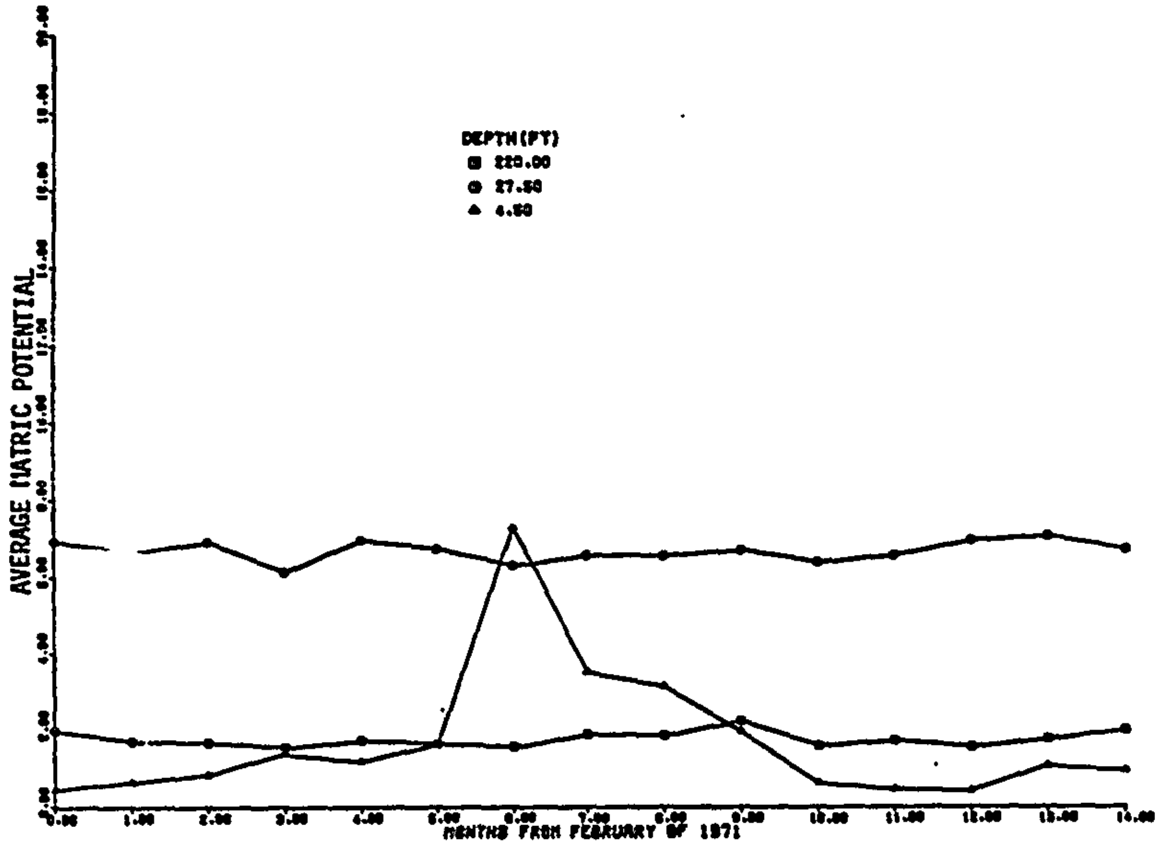

FIGURE C-8. Average Monthly Matric Potential Versus Time for Selected Psychrometer Depths

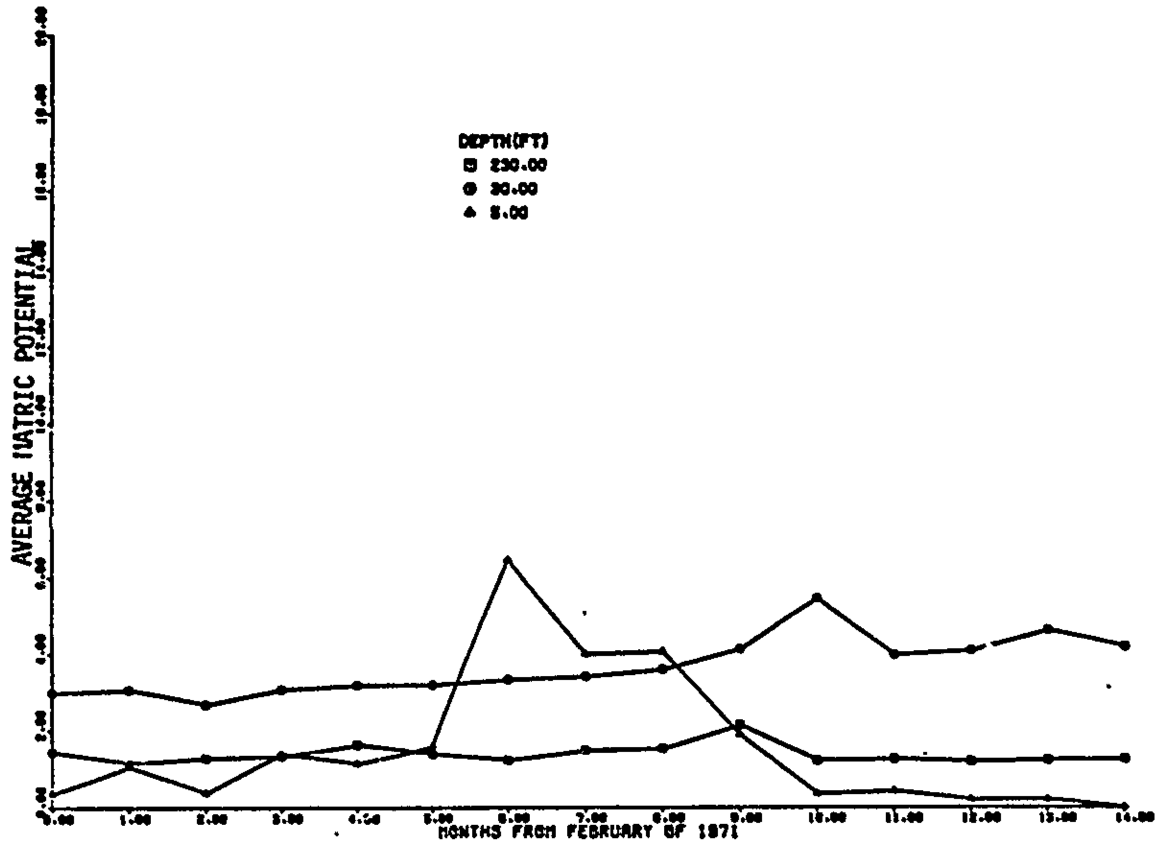

FIGURE C-9. Average Monthly Matric Potential Versus Time for Selected Psychrometer Depths

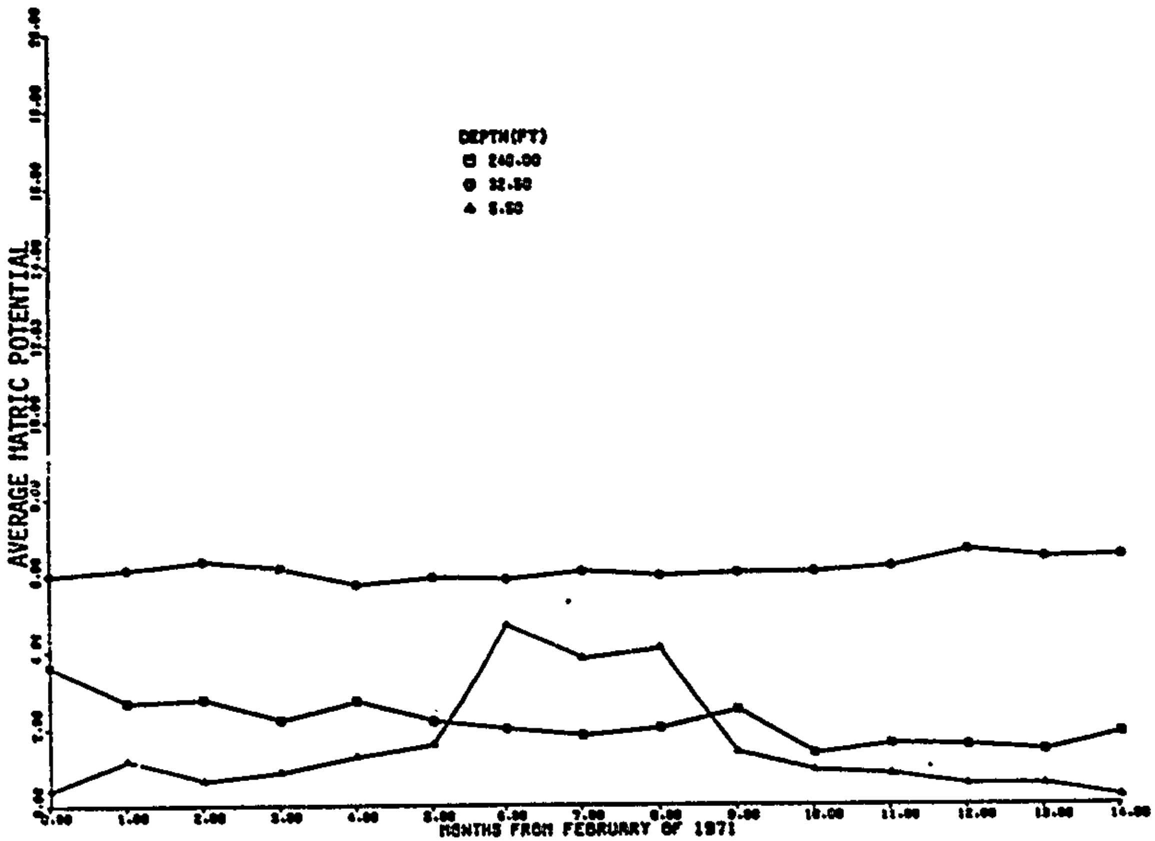

FIGURE C-10. Average Monthly Matric Potential Versus Time for Selected Psychrometer Depths

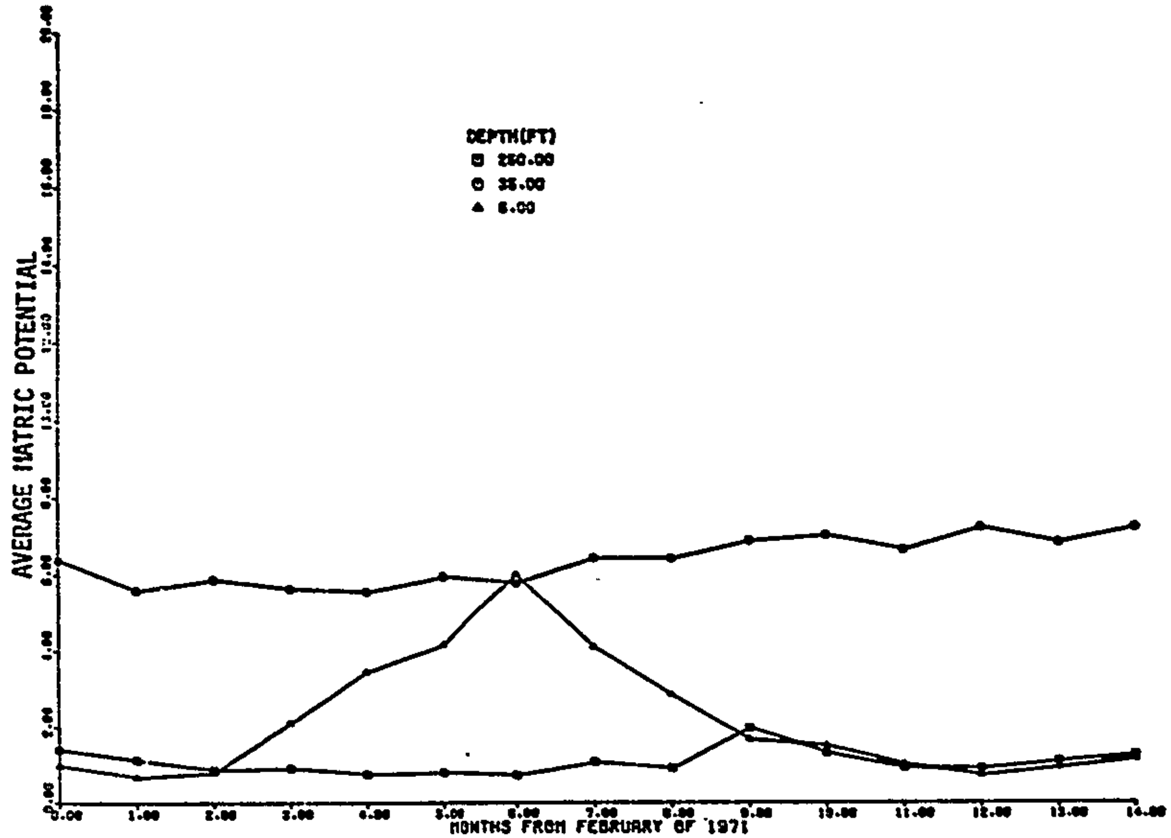

FIGURE C-11. Average Monthly Matric Potential Versus Time for Selected Psychrometer Depths

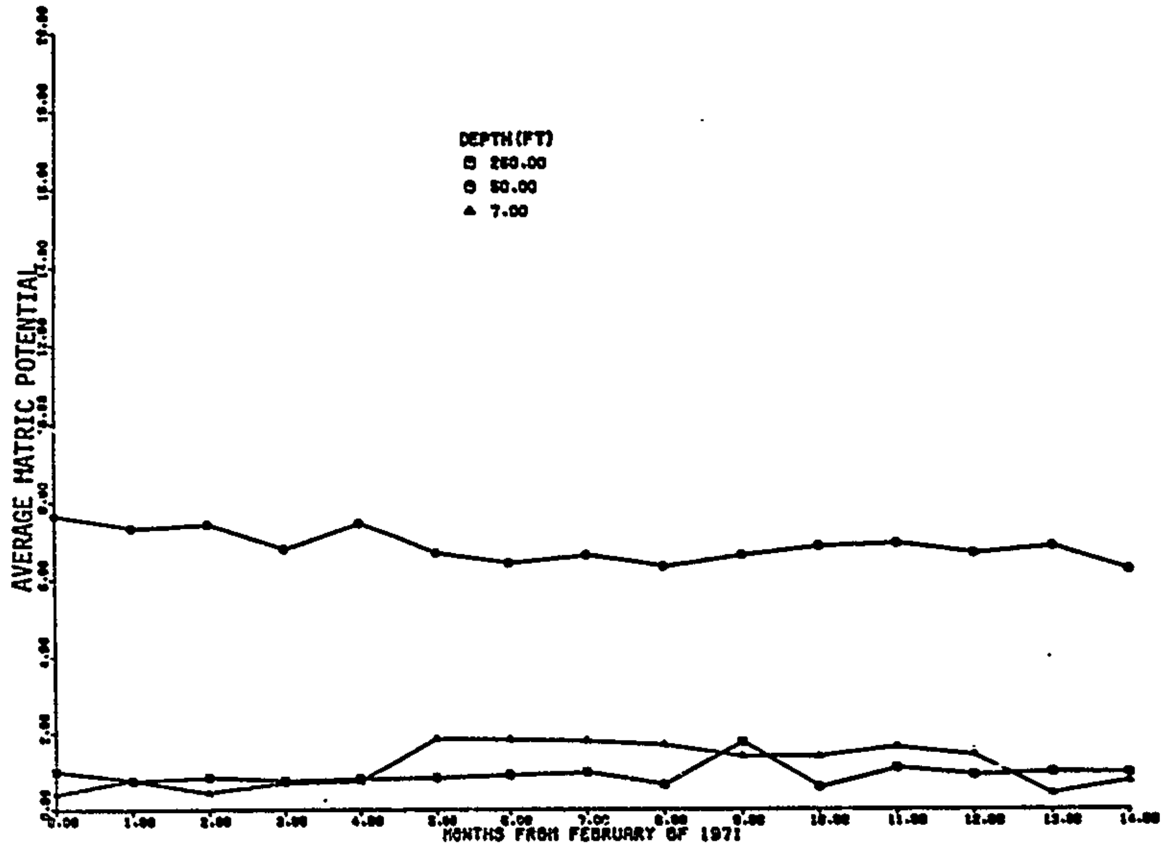

FIGURE C-12. Average Monthly Matric Potential Versus Time for Selected Psychrometer Depths

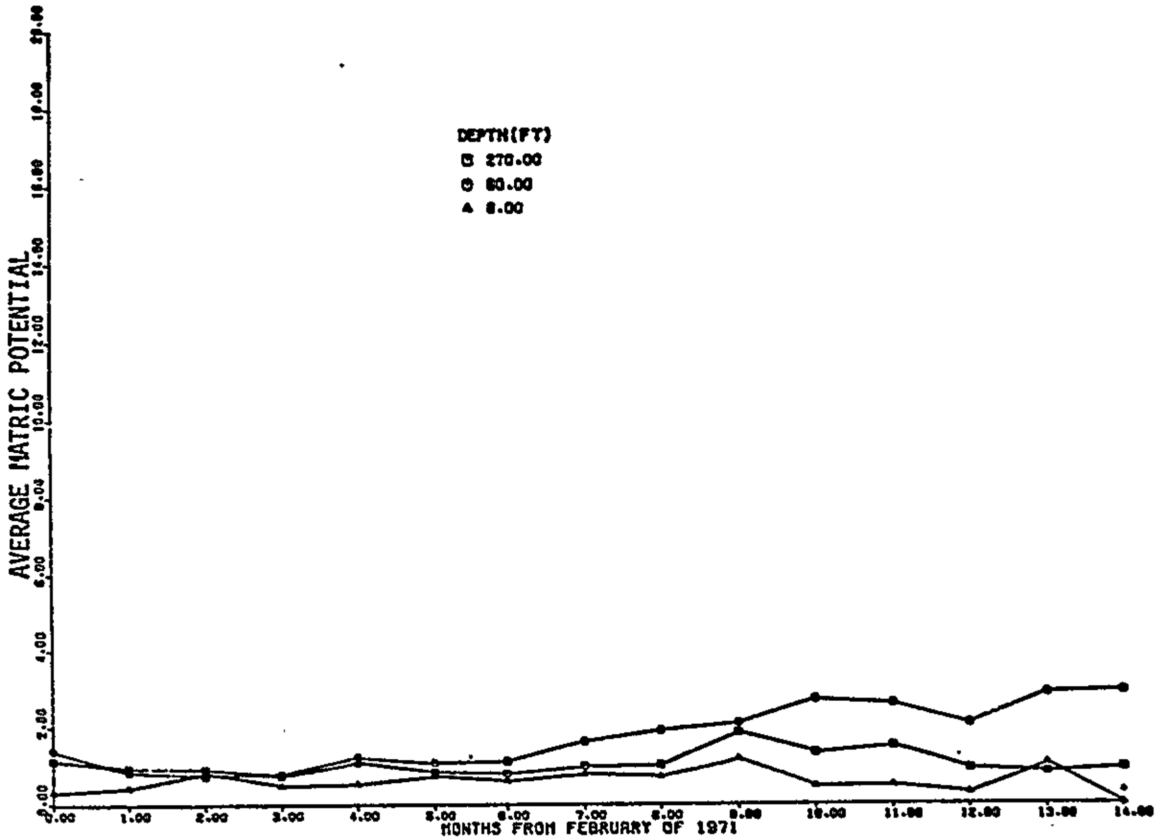

FIGURE C-13. Average Monthly Matric Potential Versus Time for Selected Psychrometer Depths

9312972 364

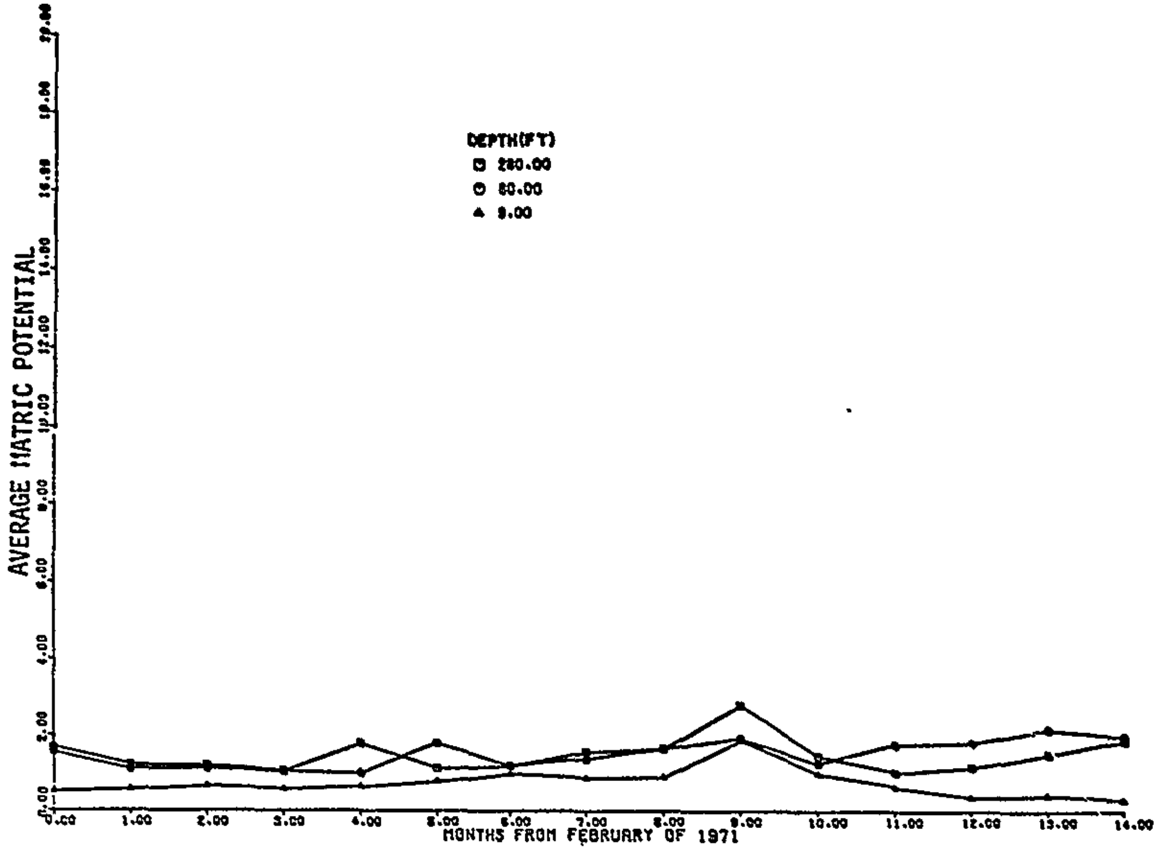

FIGURE C-14. Average Monthly Matric Potential Versus Time for Selected Psychrometer Depths

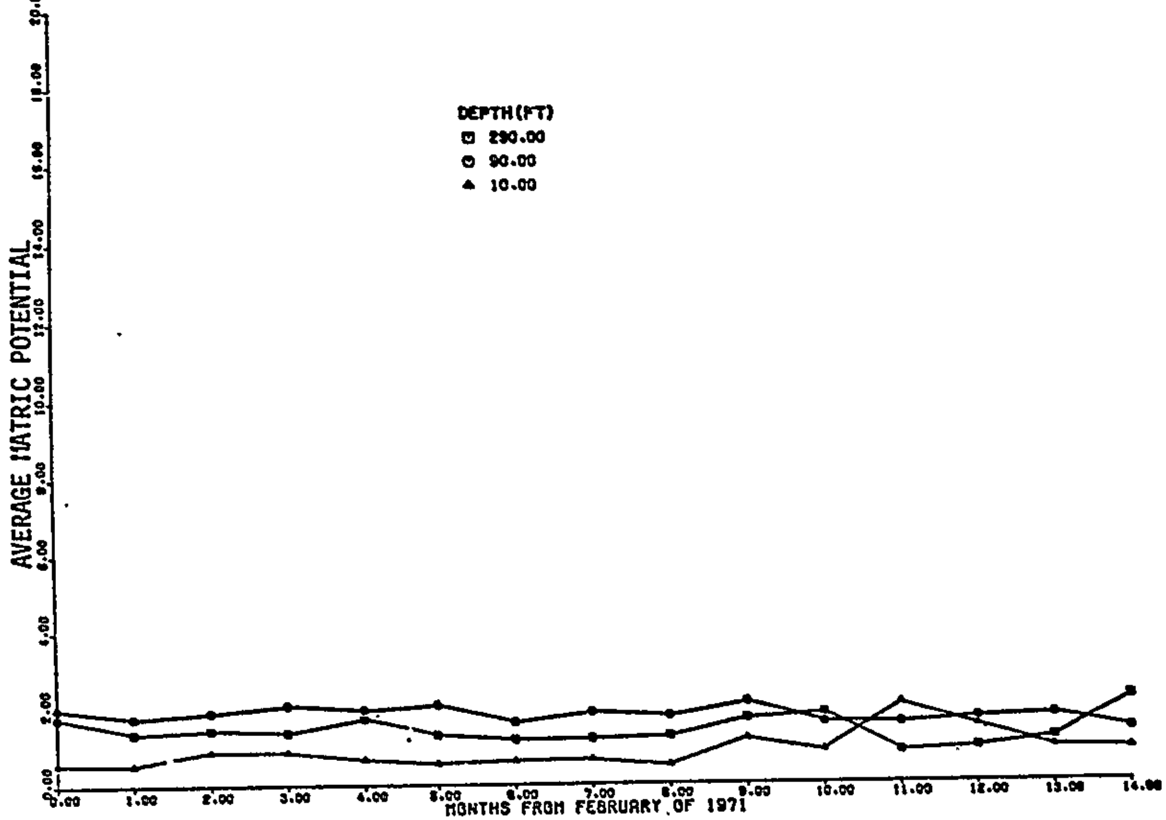

FIGURE C-15. Average Monthly Matric Potential Versus Time for Selected Psychrometer Depths

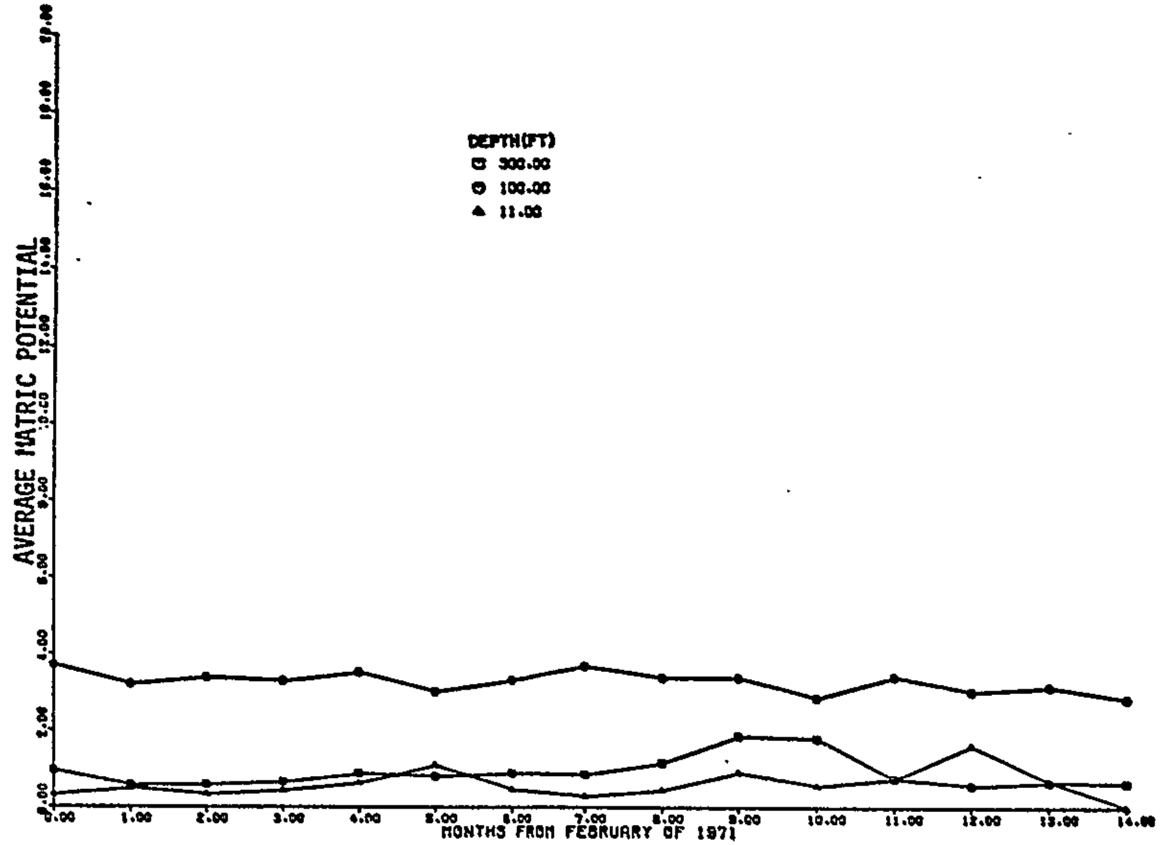

FIGURE C-16. Average Monthly Matric Potential Versus Time for Selected Psychrometer Depths

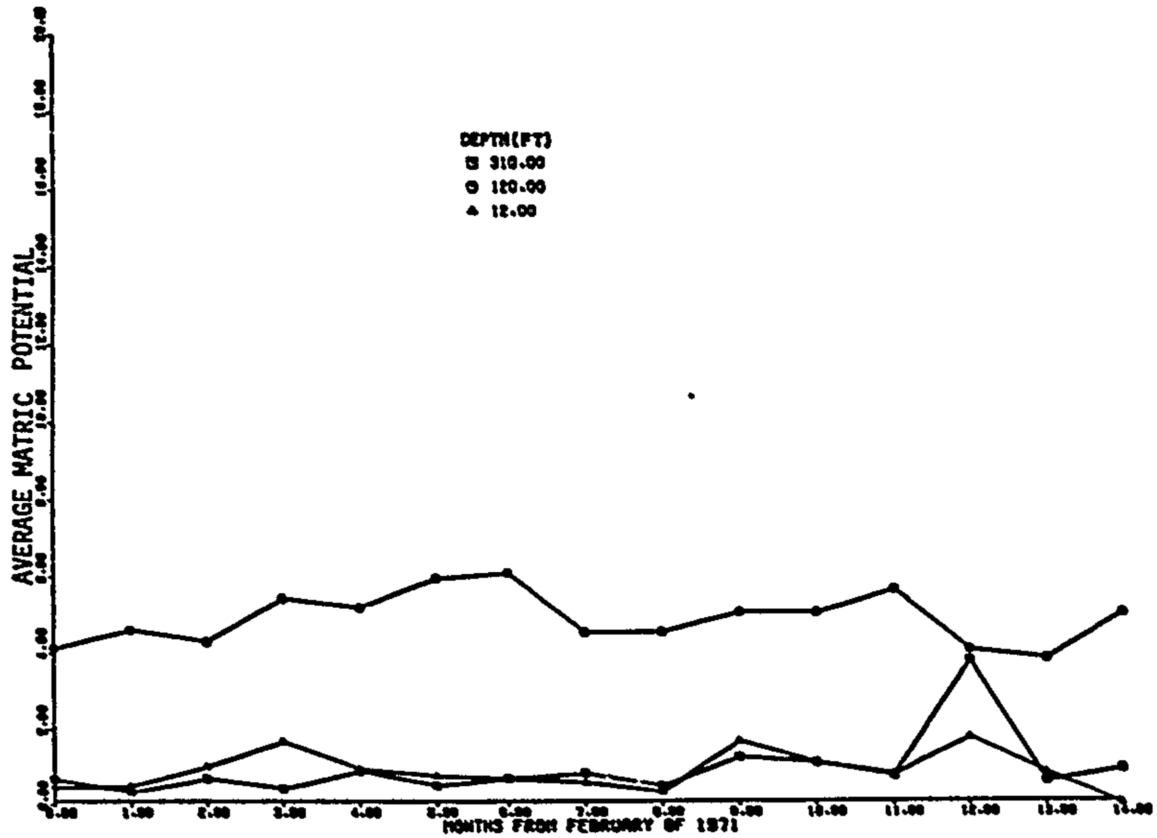

FIGURE C-17. Average Monthly Matric Potential Versus Time for Selected Psychrometer Depths

APPENDIX D

AVERAGE MEASURED MONTHLY SOIL TEMPERATURES FOR SELECTED DEPTHS

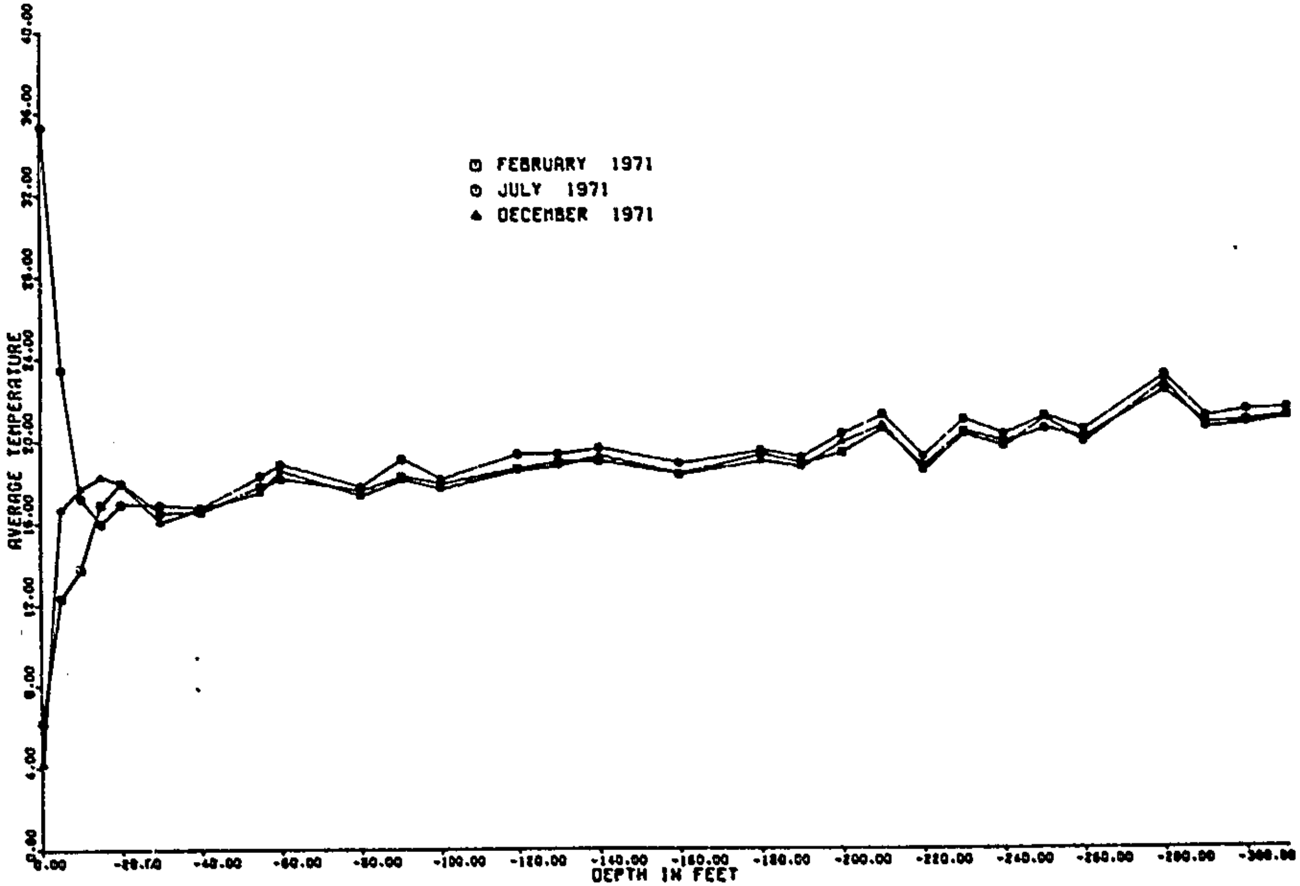

FIGURE D-1. Average Measured Monthly Soil Temperature as a Function of Depth for Selected Month

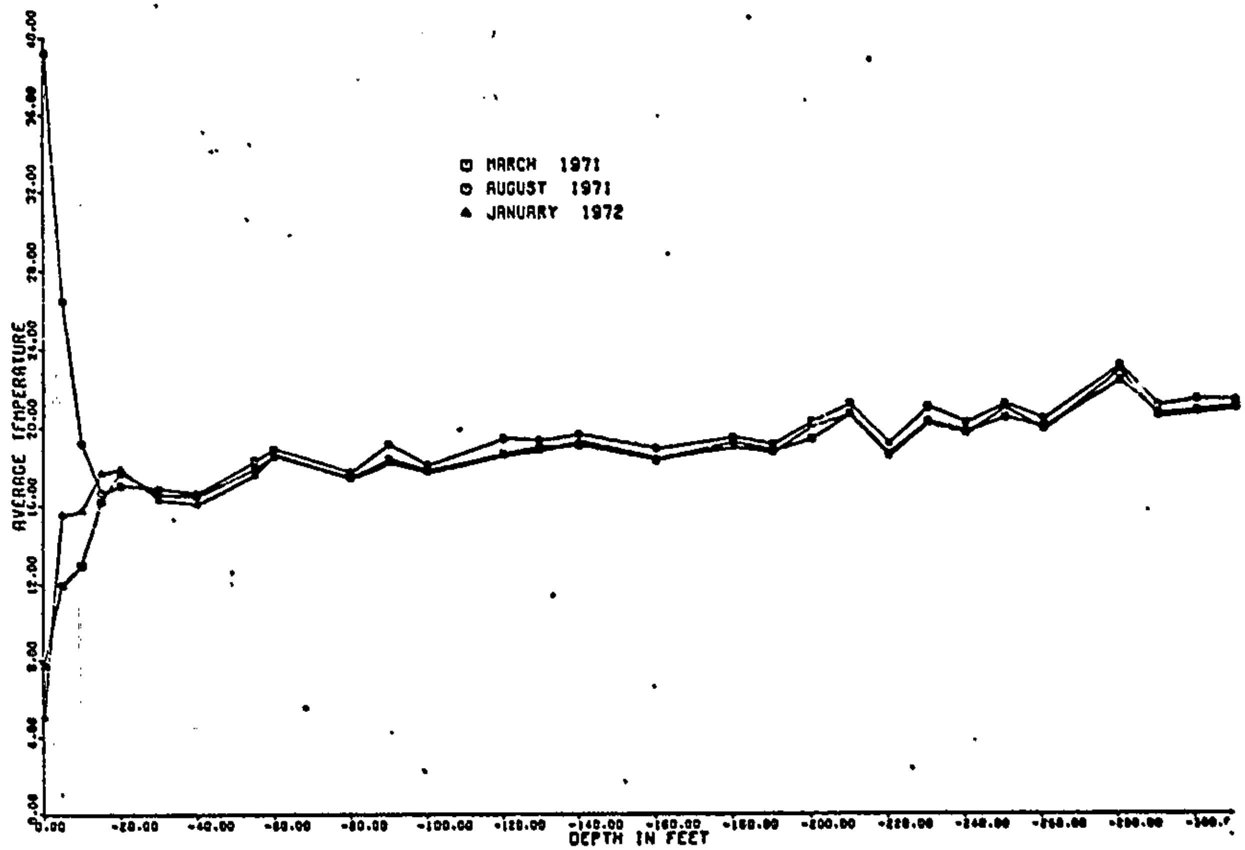

FIGURE D-2. Average Measured Monthly Soil Temperature as a Function of Depth for Selected Month

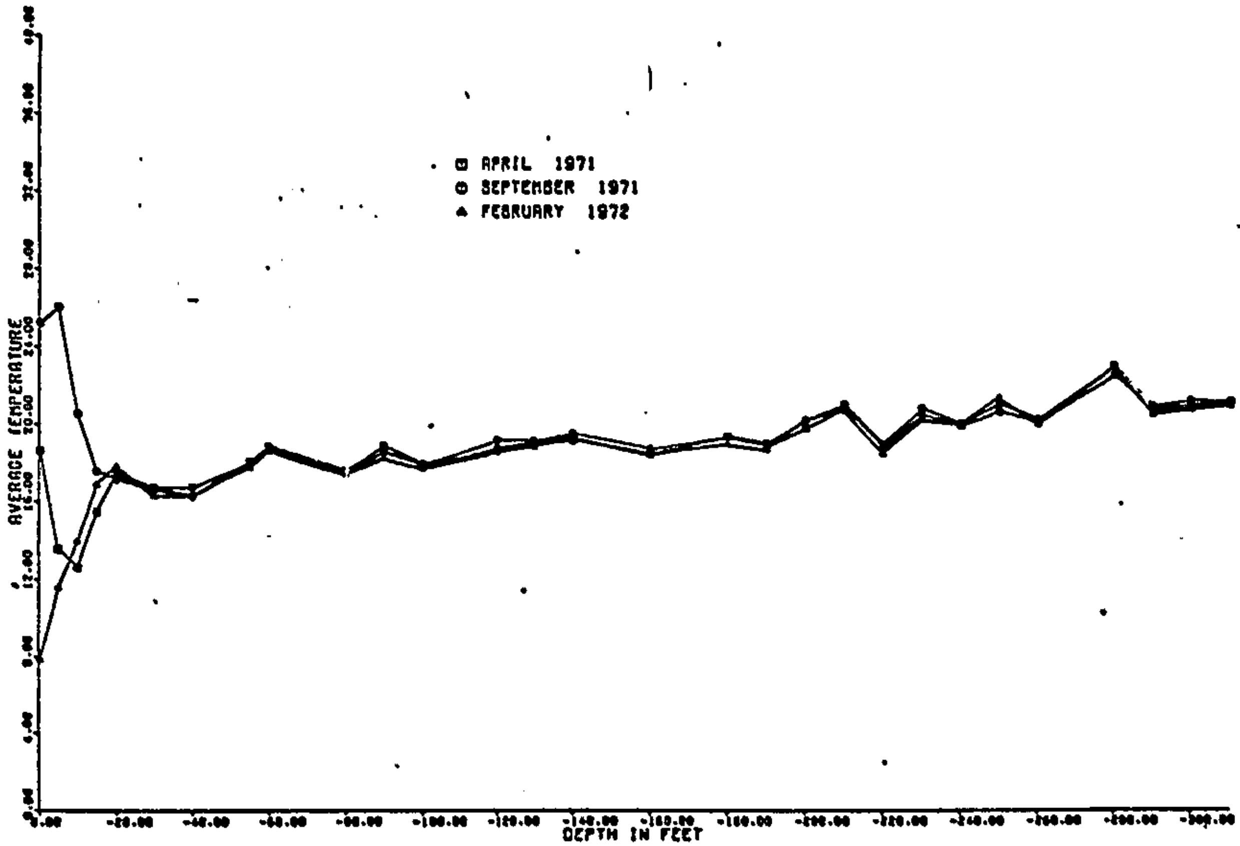

FIGURE D-3. Average Measured Monthly Soil Temperature as a Function of Depth for Selected Month

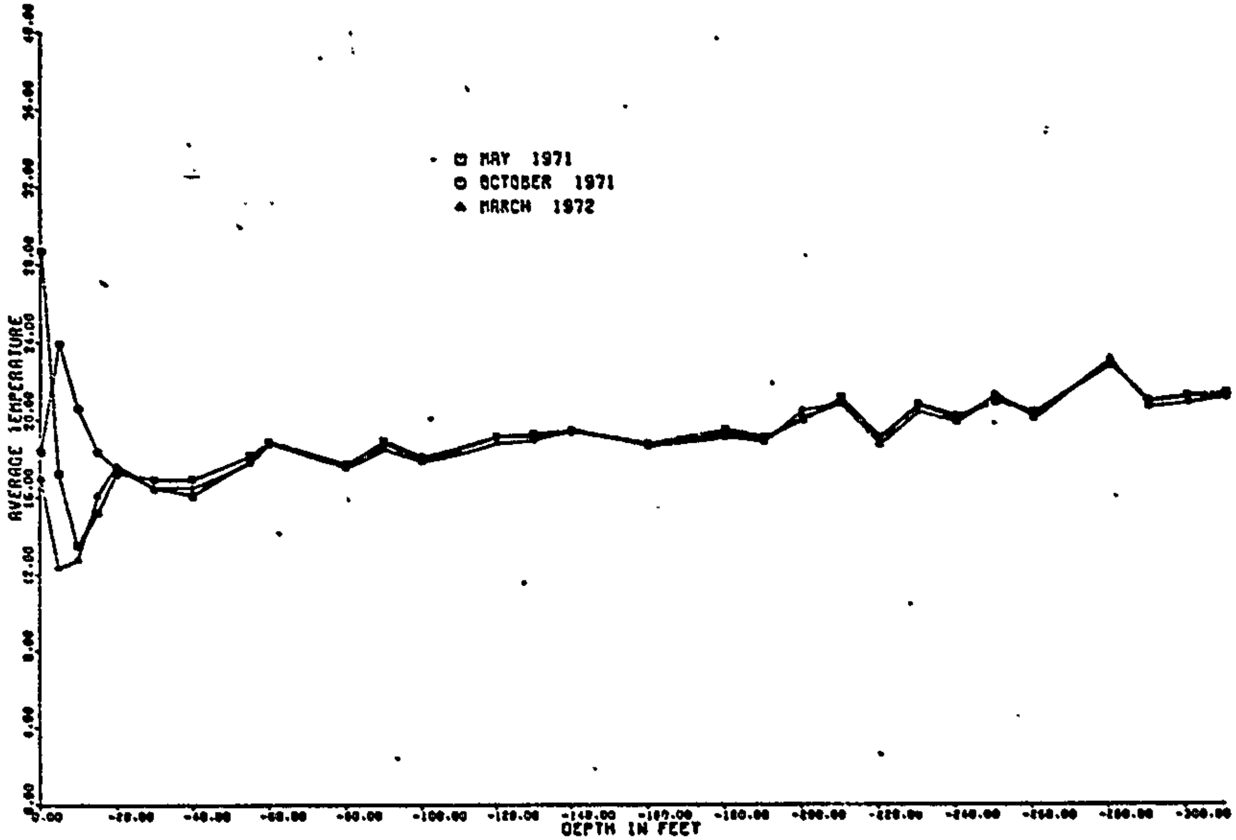

FIGURE D-4. Average Measured Monthly Soil Temperature as a Function of Depth for Selected Month

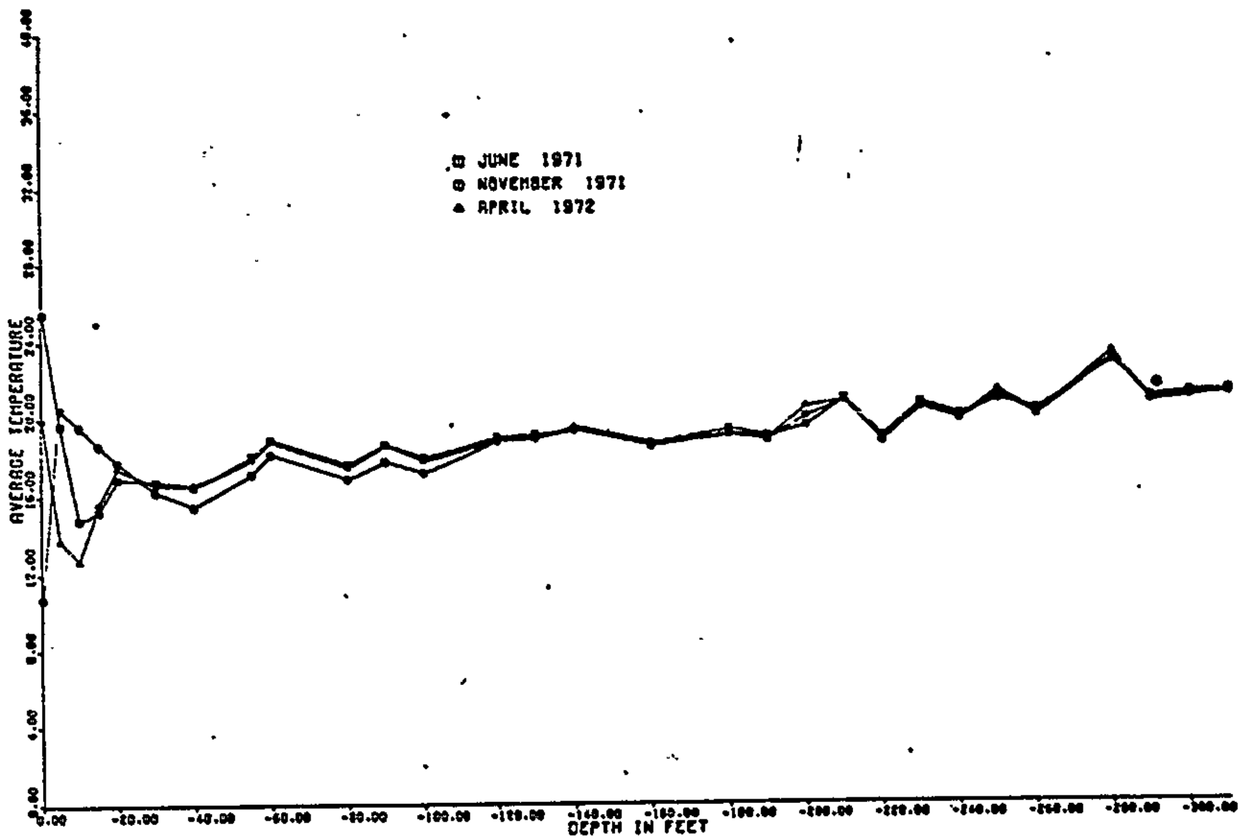

FIGURE D-5. Average Measured Monthly Soil Temperature as a Function of Depth for Selected Month

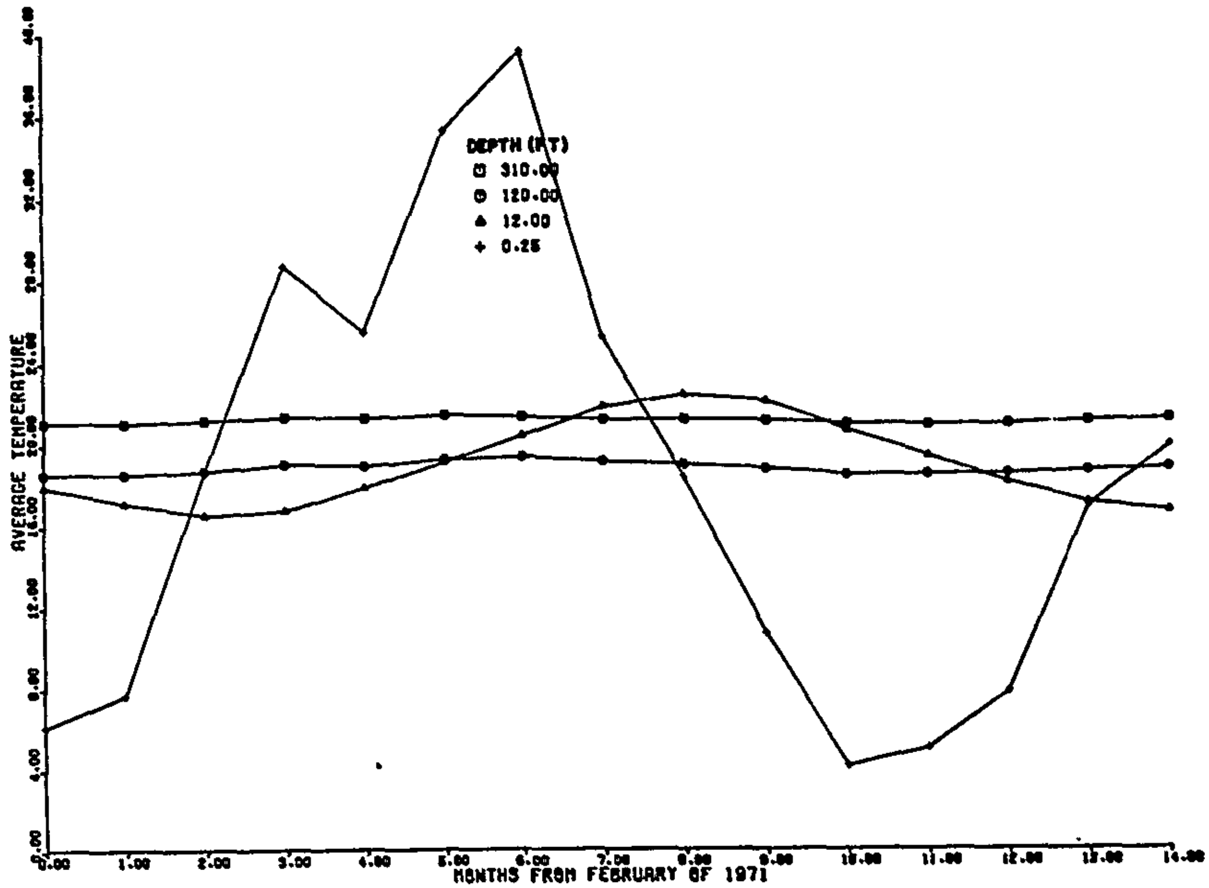

FIGURE D-6. Average Measured Monthly Soil Temperature (°C) Versus Time for Selected Depths

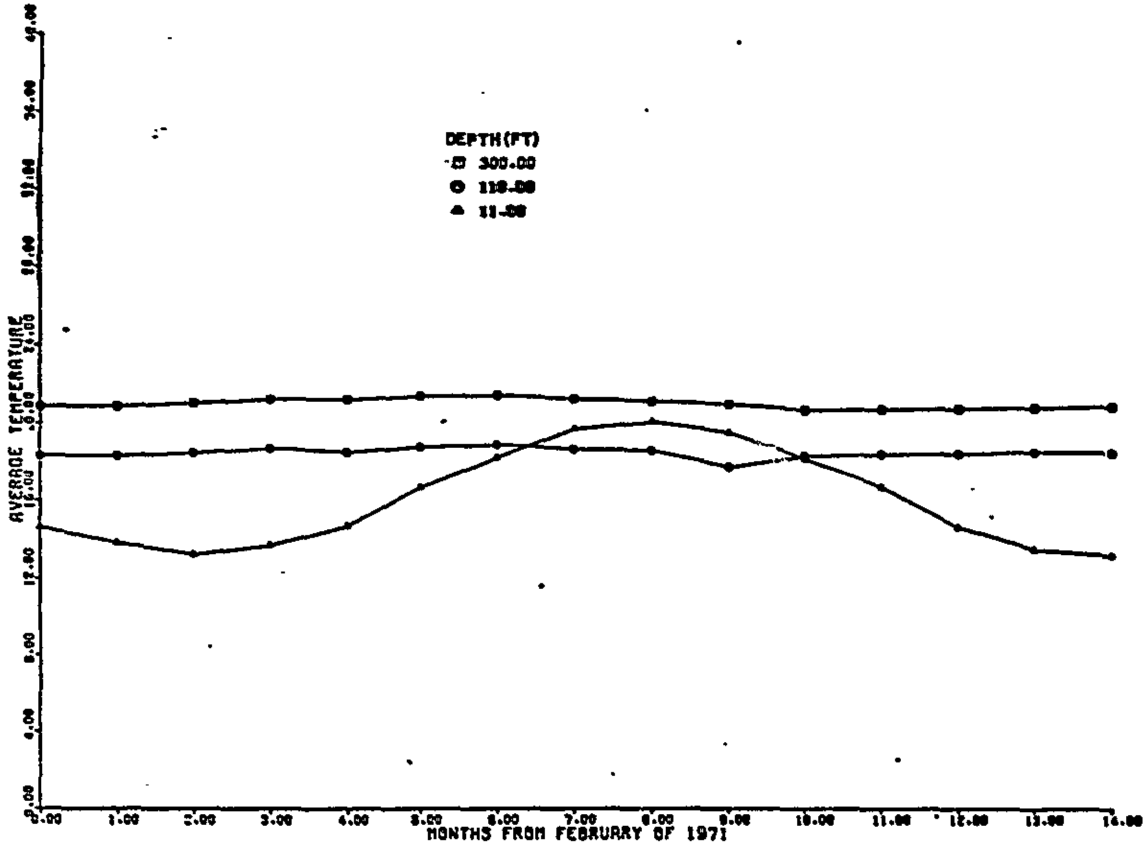

FIGURE D-7. Average Measured Monthly Soil Temperature (°C) Versus Time for Selected Depths

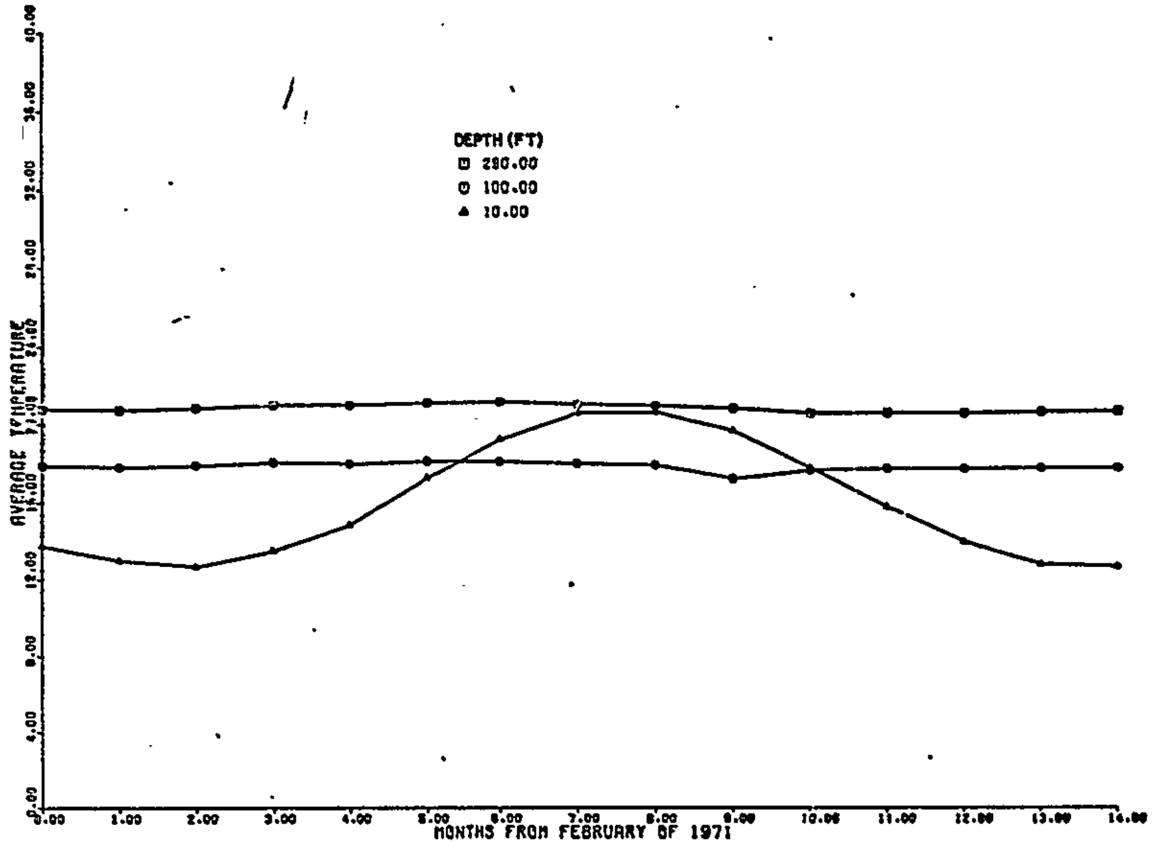

FIGURE D-8. Average Measured Monthly Soil Temperature (°C) Versus Time for Selected Depths

9 3 1 2 8 7 2 0 3 7 7

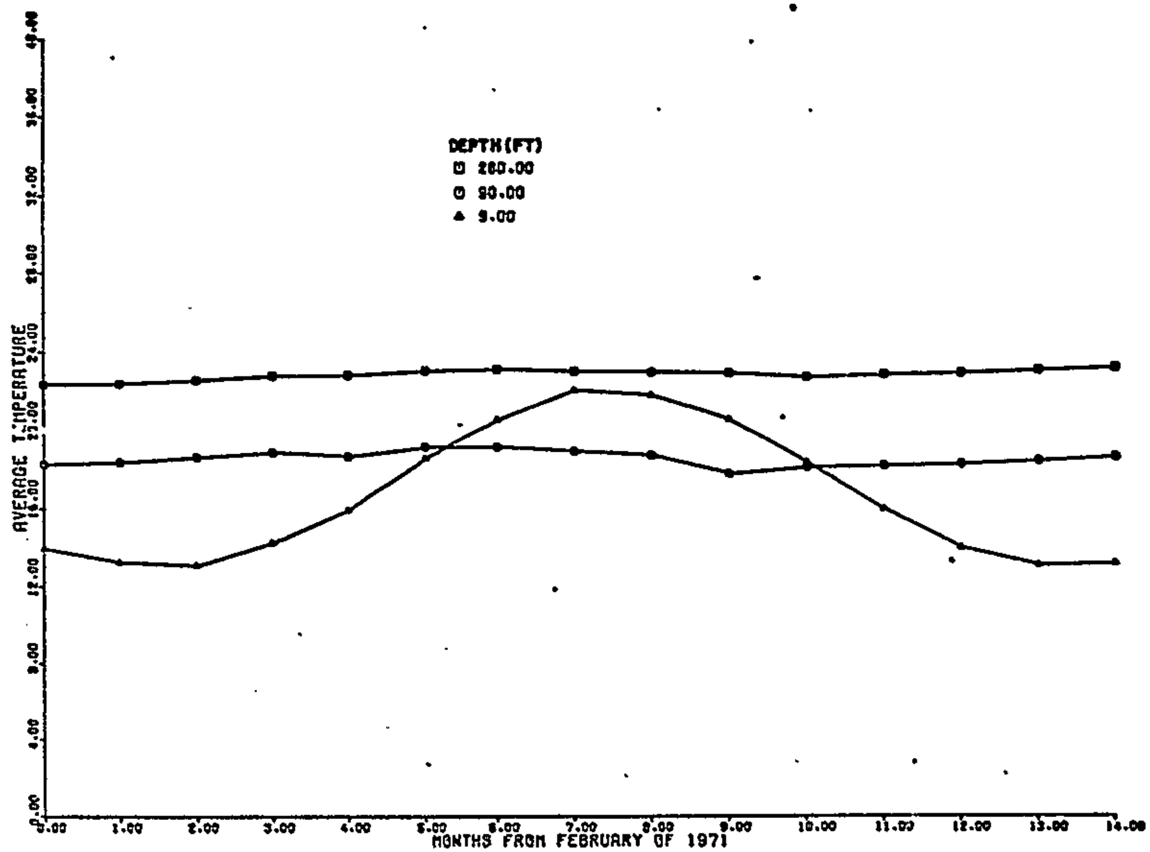

FIGURE D-9. Average Measured Monthly Soil Temperature (°C) Versus Time for Selected Depths

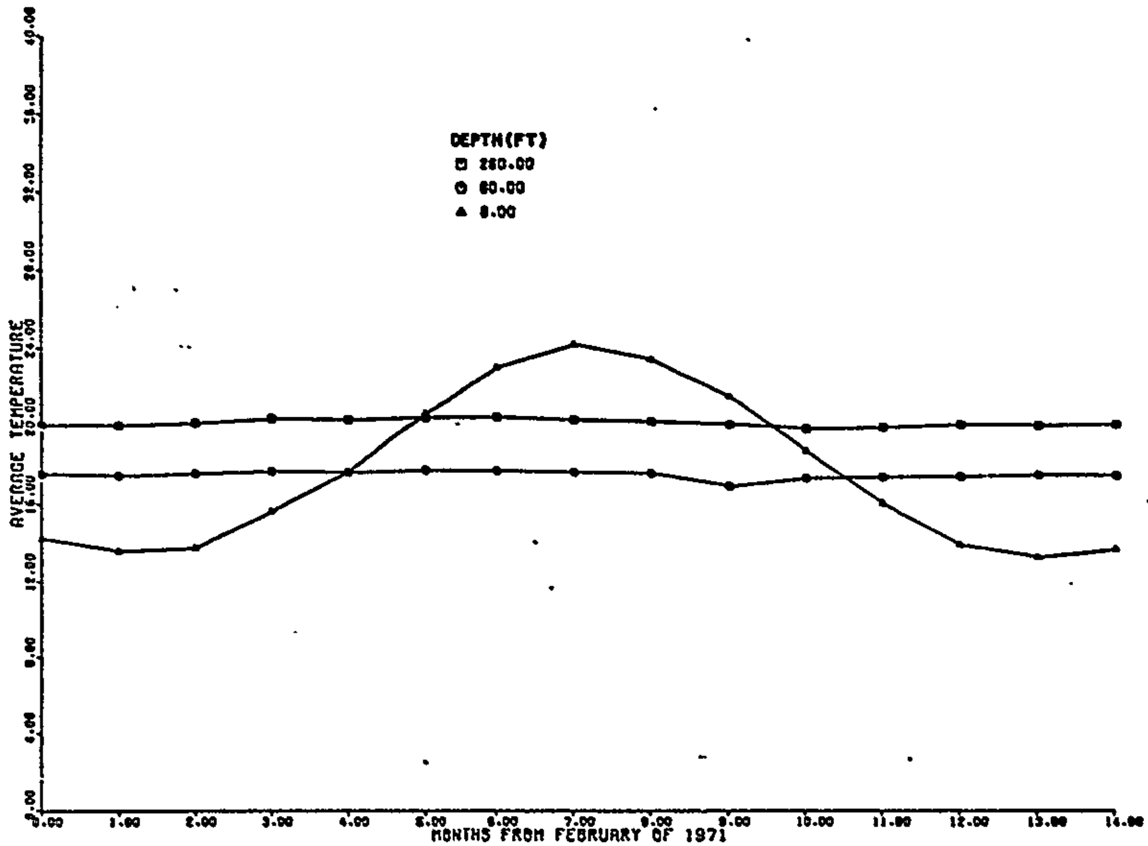

FIGURE D-10. Average Measured Monthly Soil Temperature (°C) Versus Time for Selected Depths

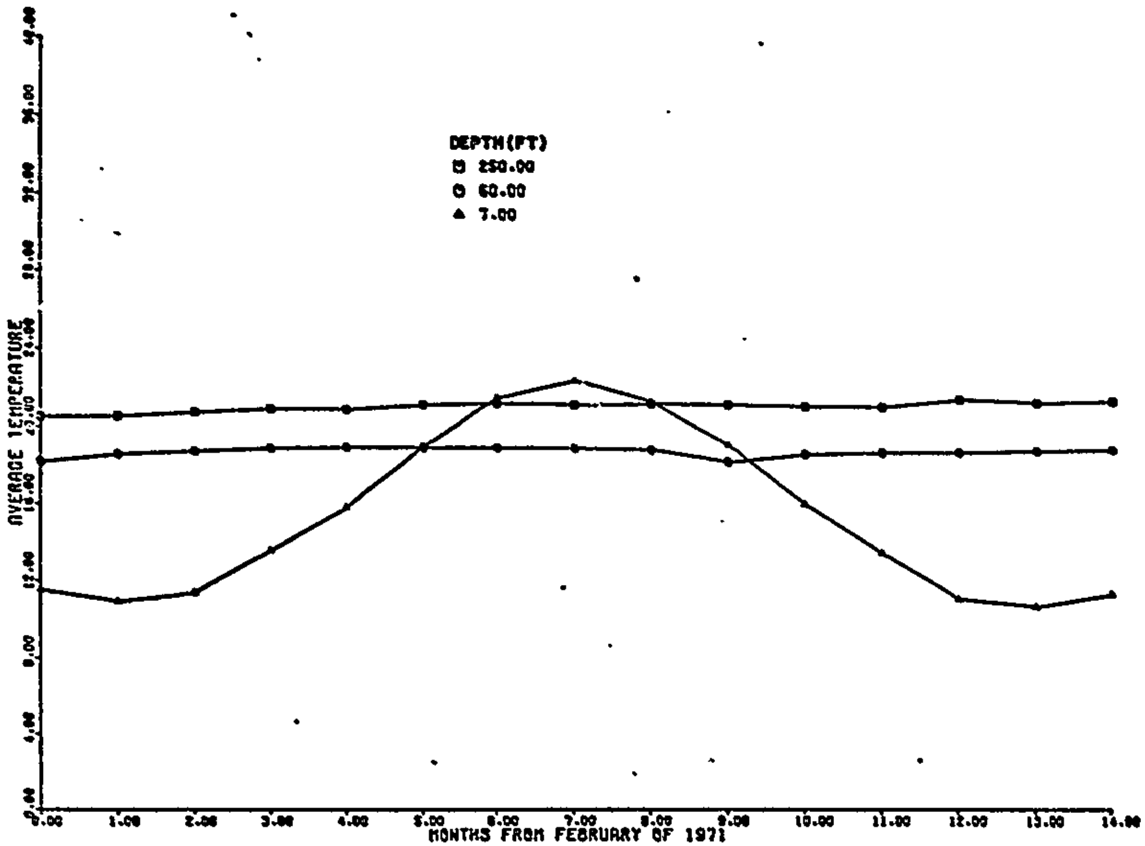

FIGURE D-11. Average Measured Monthly Soil Temperature (°C) Versus Time for Selected Depths

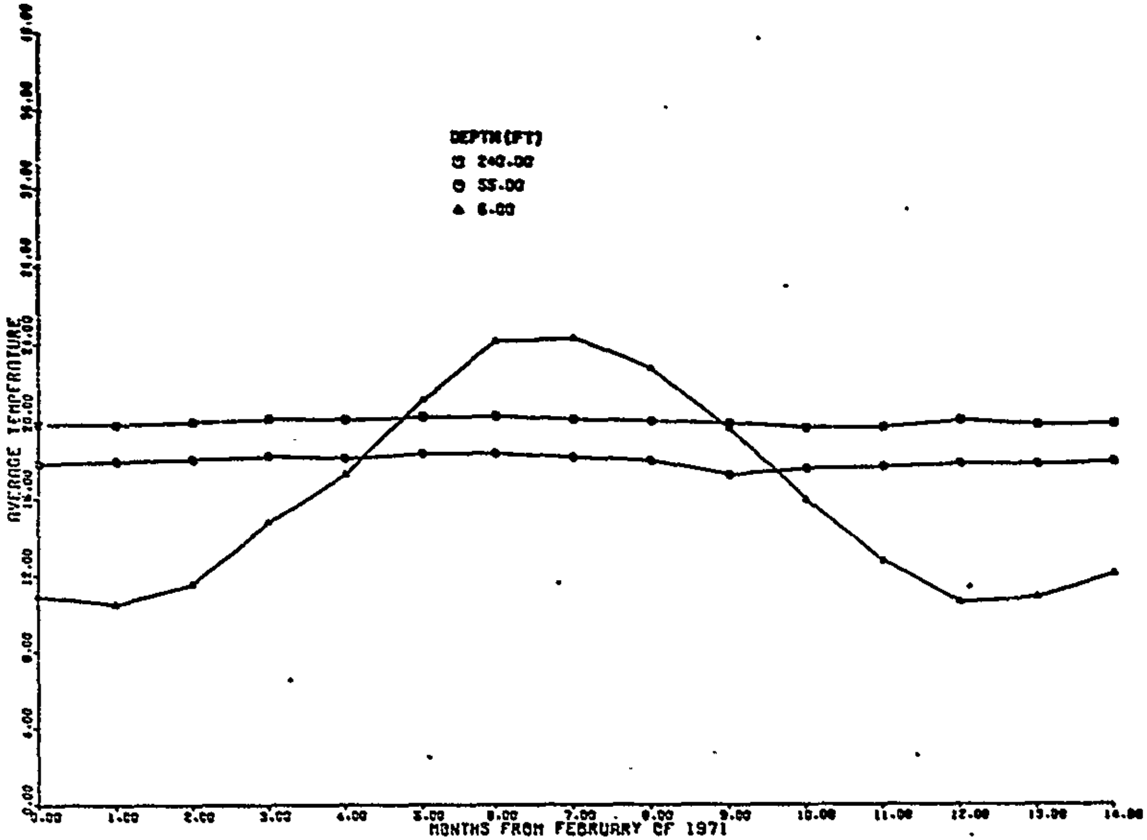

FIGURE D-12. Average Measured Monthly Soil Temperature (°C) Versus Time for Selected Depths

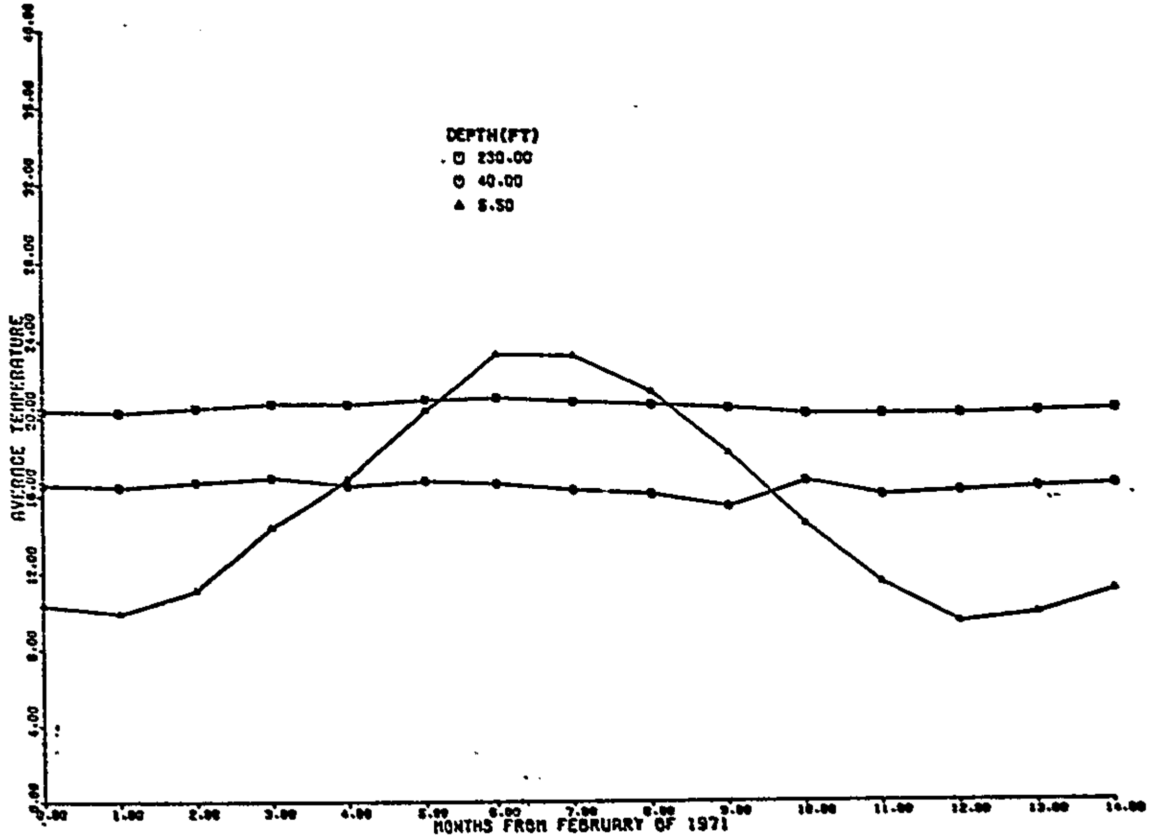

FIGURE D-13. Average Measured Monthly Soil Temperature (°C) Versus Time for Selected Depths

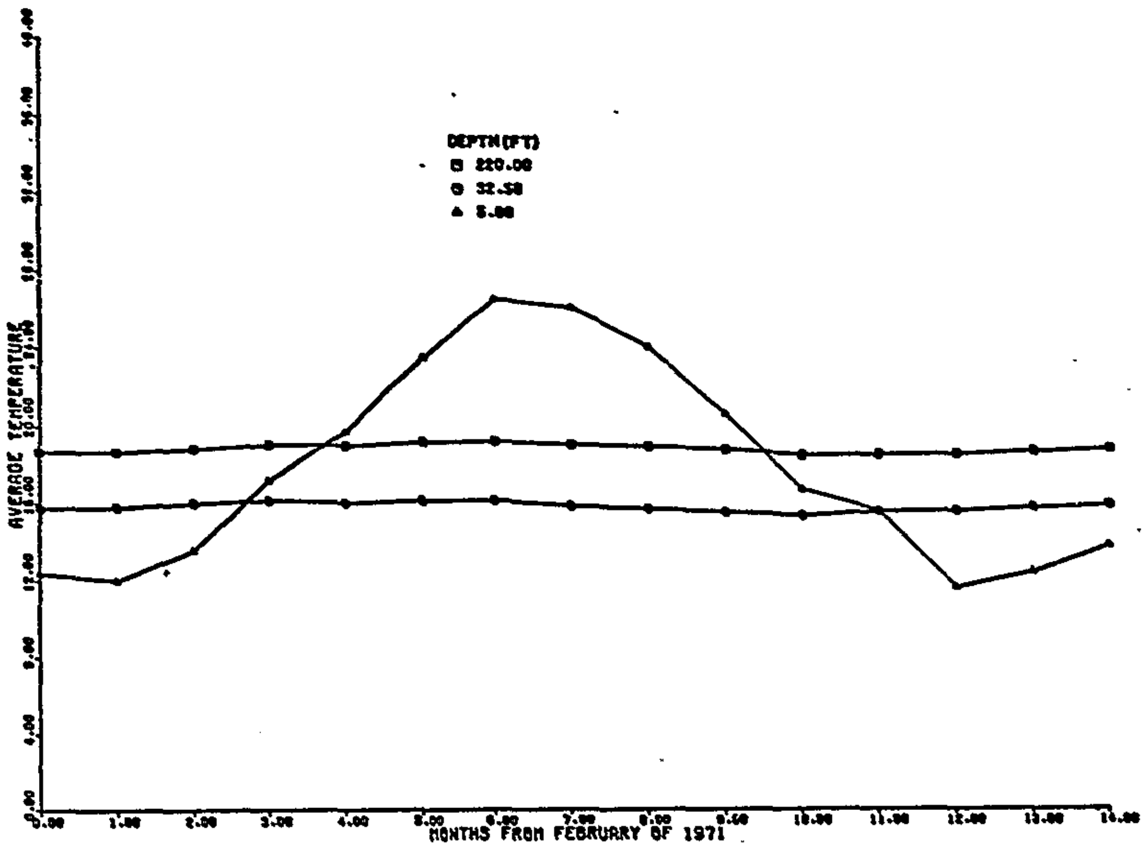

FIGURE D-14. Average Measured Monthly Soil Temperature (°C) Versus Time for Selected Depths

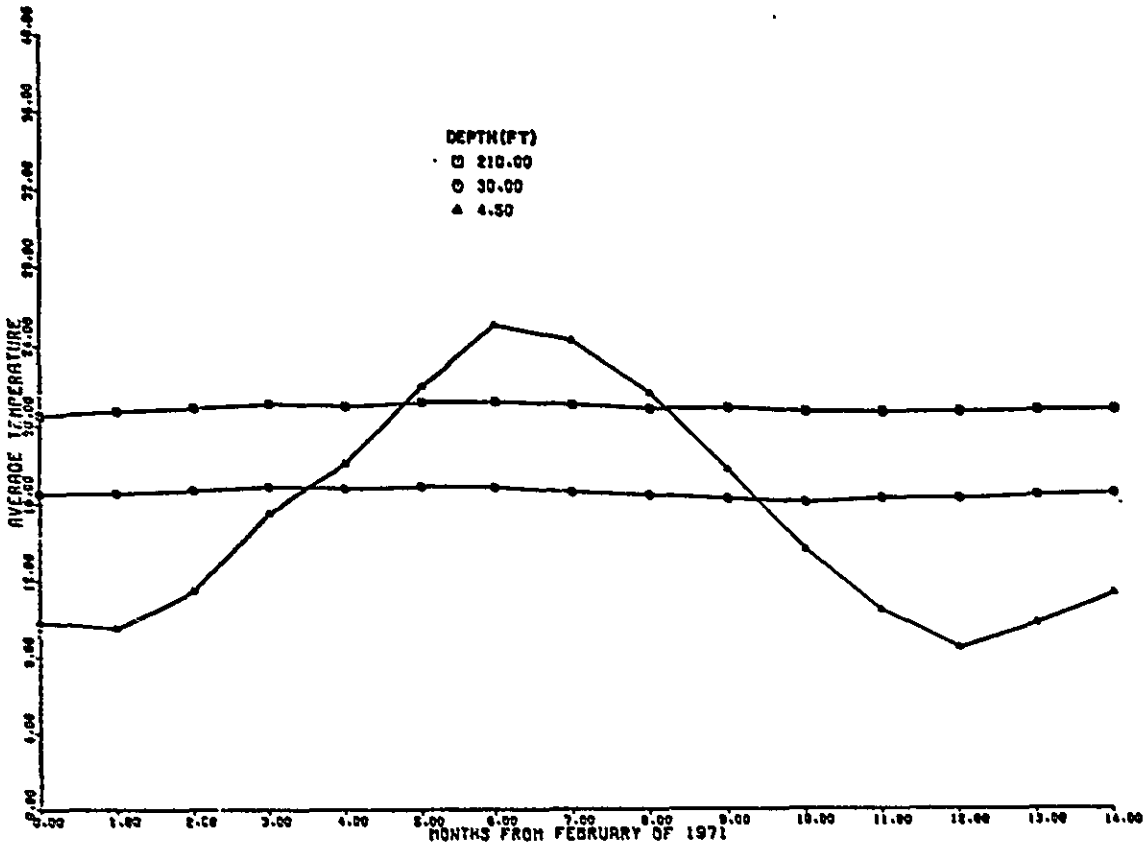

FIGURE D-15. Average Measured Monthly Soil Temperature (°C) Versus Time for Selected Depths

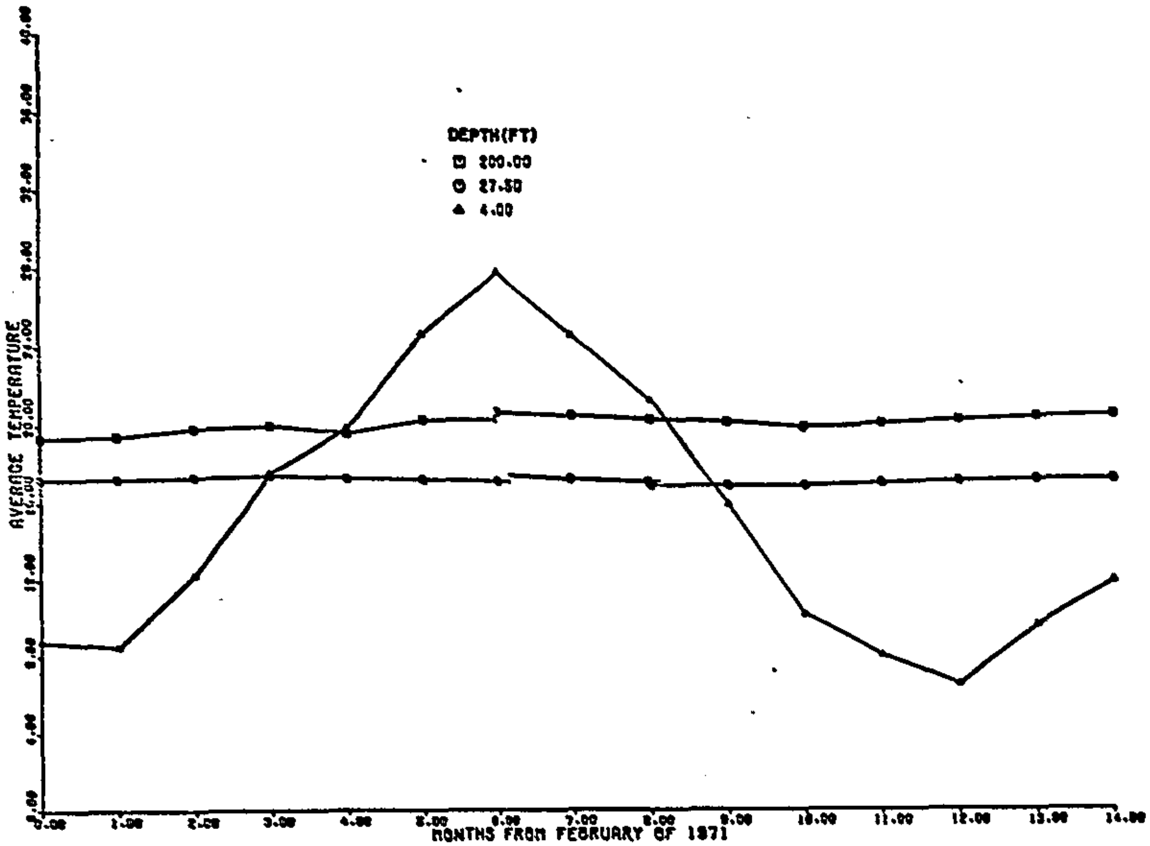

FIGURE D-16. Average Measured Monthly Soil Temperature (°C) Versus Time for Selected Depths

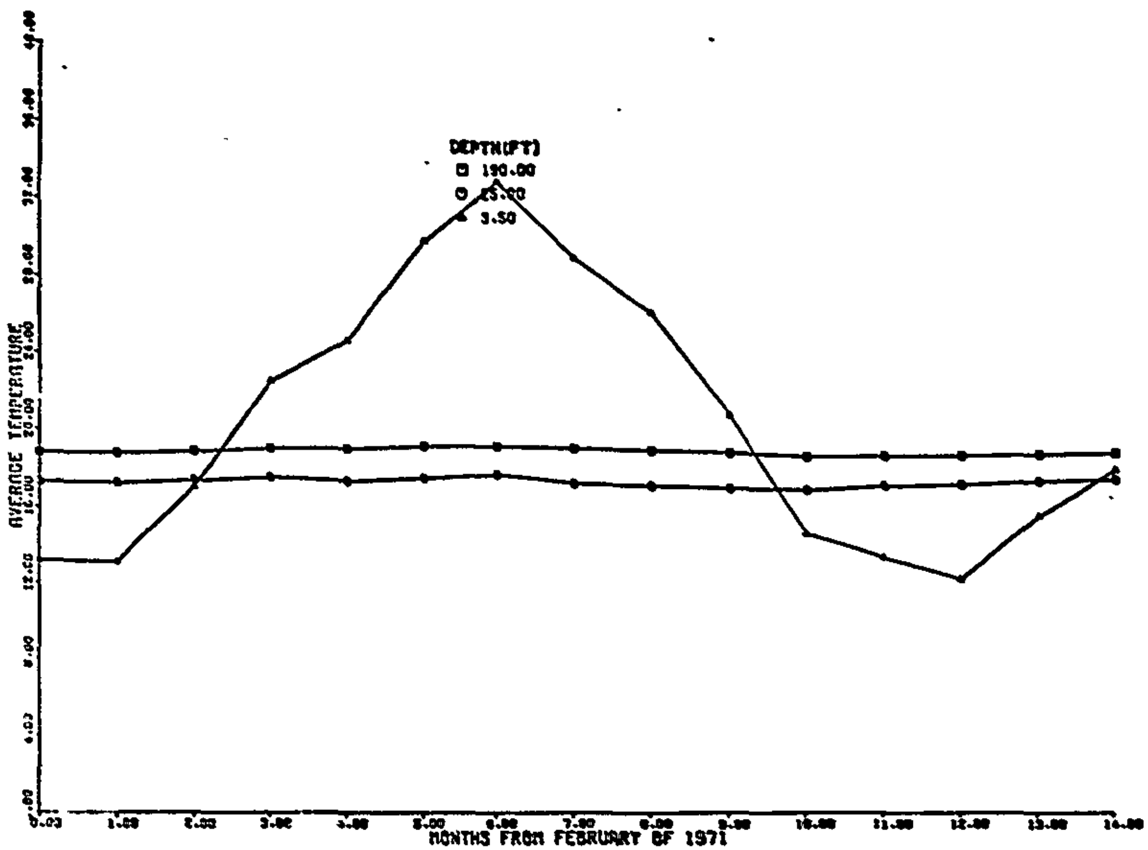

FIGURE D-17. Average Measured Monthly Soil Temperature (°C) Versus Time for Selected Depths

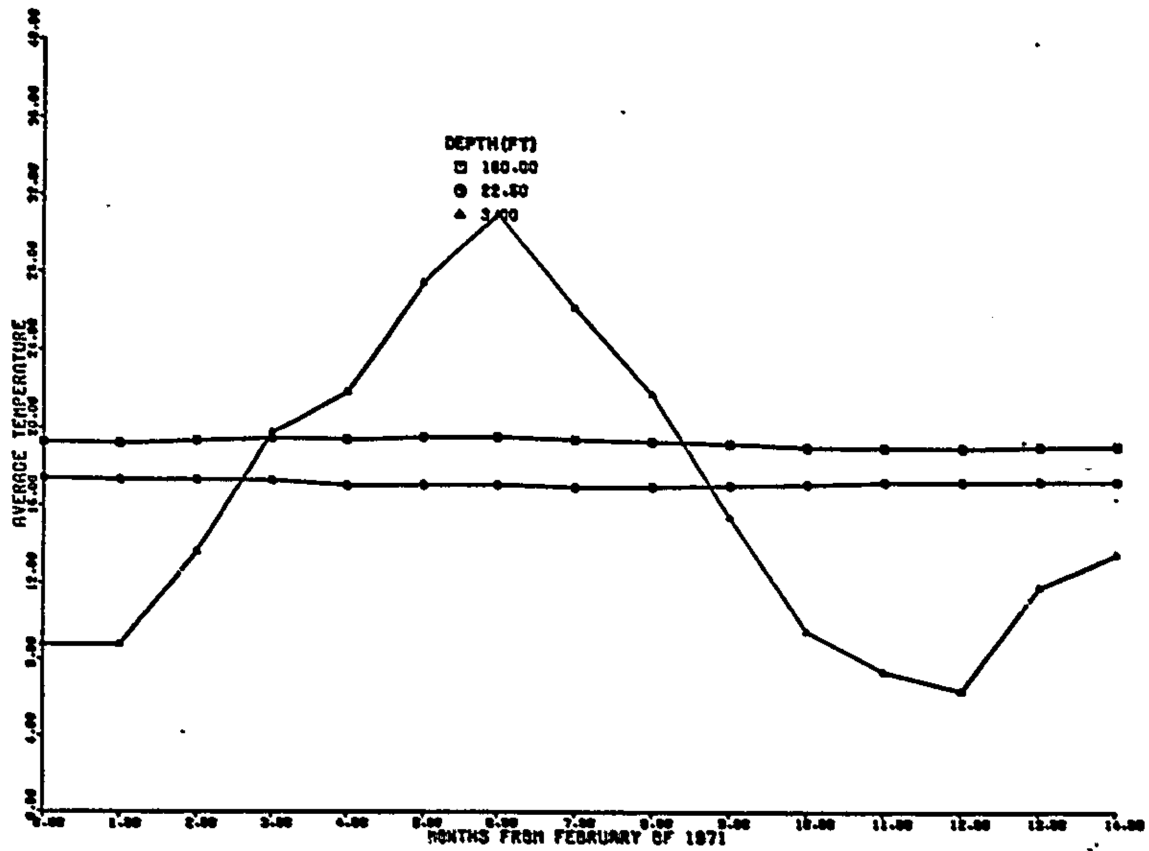

FIGURE D-18. Average Measured Monthly Soil Temperature (°C) Versus Time for Selected Depths

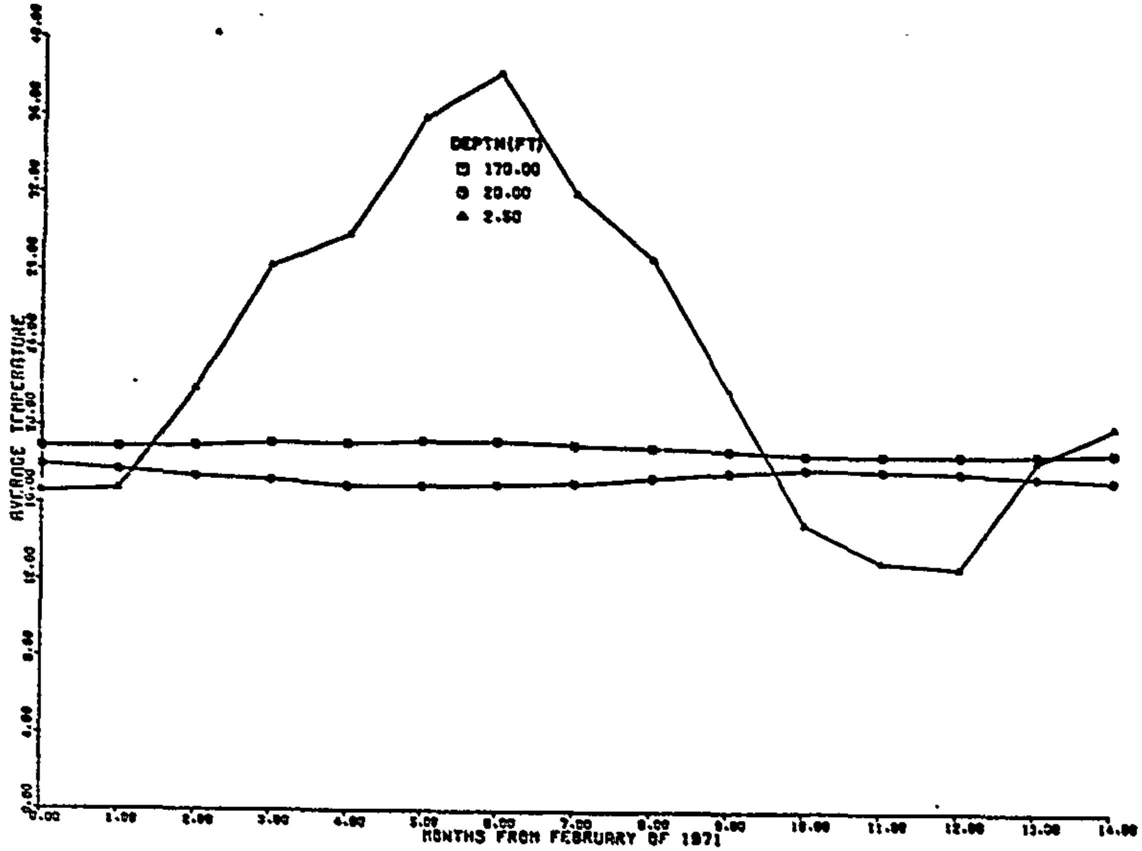

FIGURE D-19. Average Measured Monthly Soil Temperature (°C) Versus Time for Selected Depths

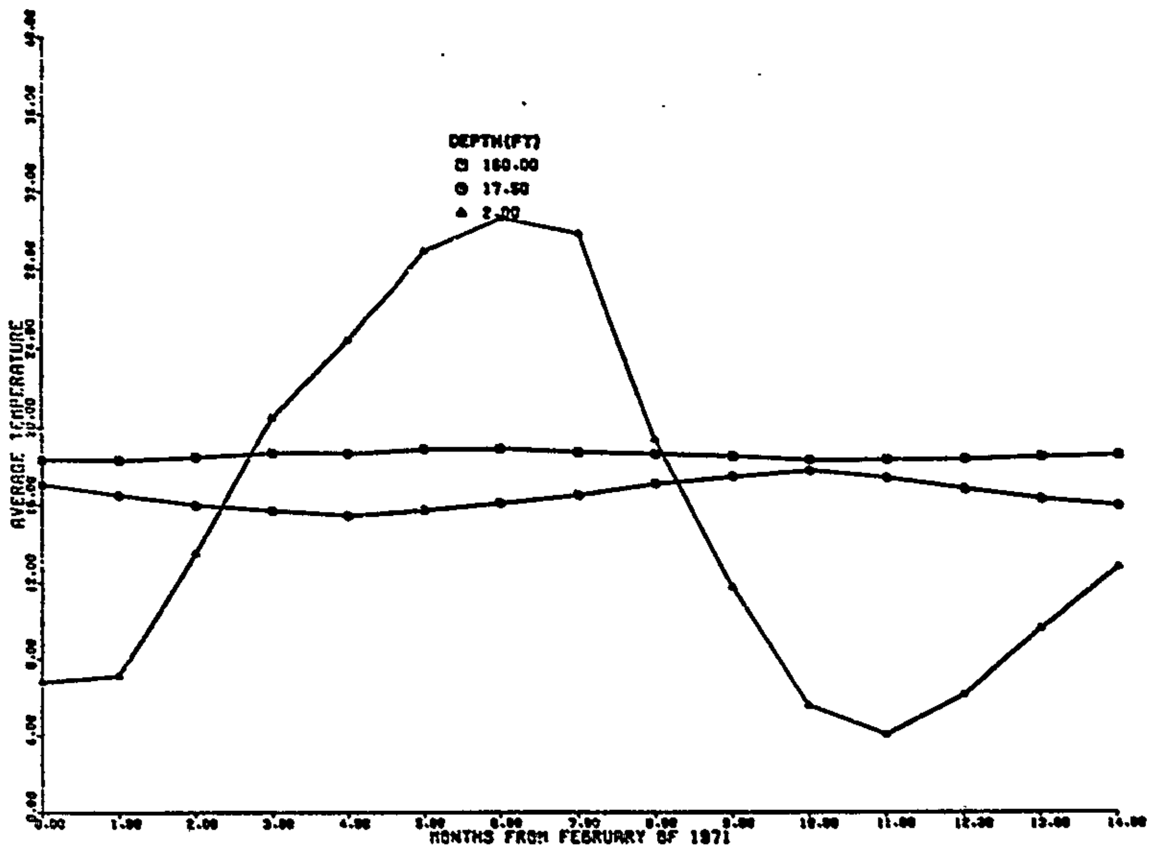

FIGURE D-20. Average Measured Monthly Soil Temperature (°C) Versus Time for Selected Depths

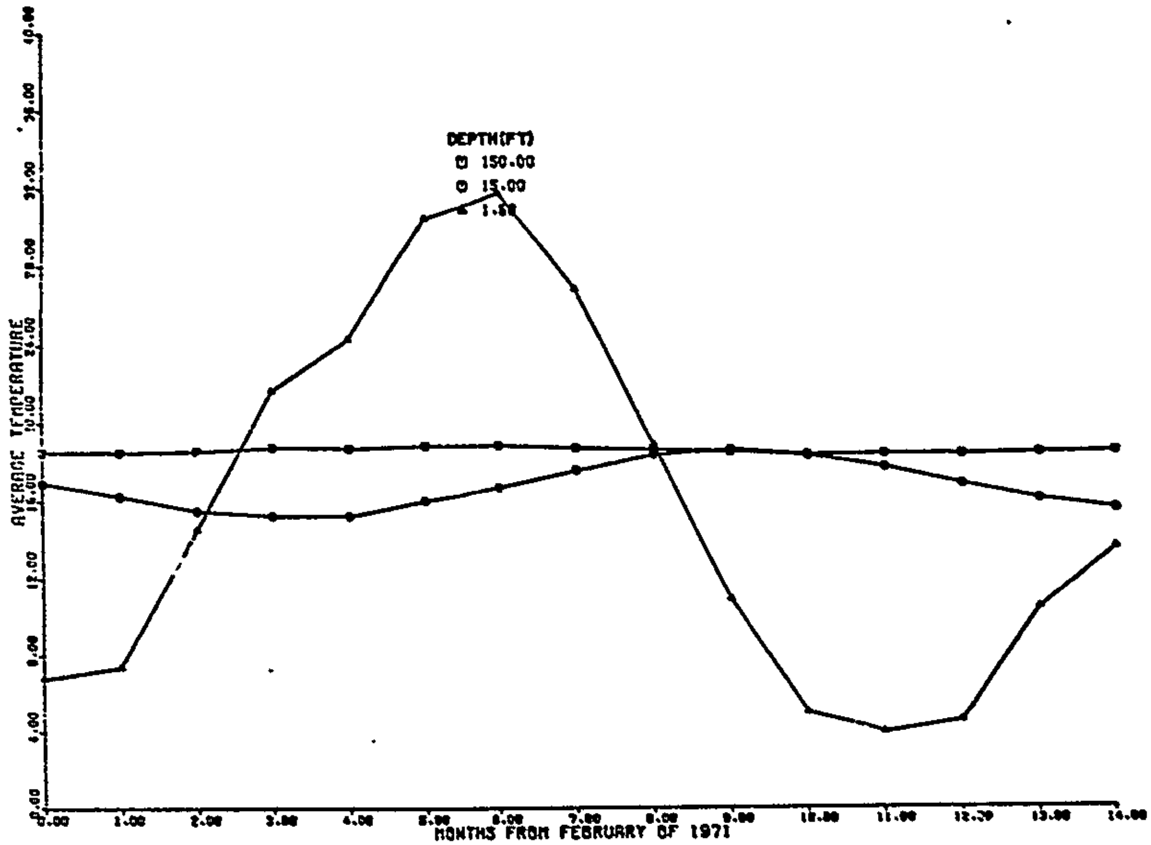

FIGURE D-21. Average Measured Monthly Soil Temperature (°C) Versus Time for Selected Depths

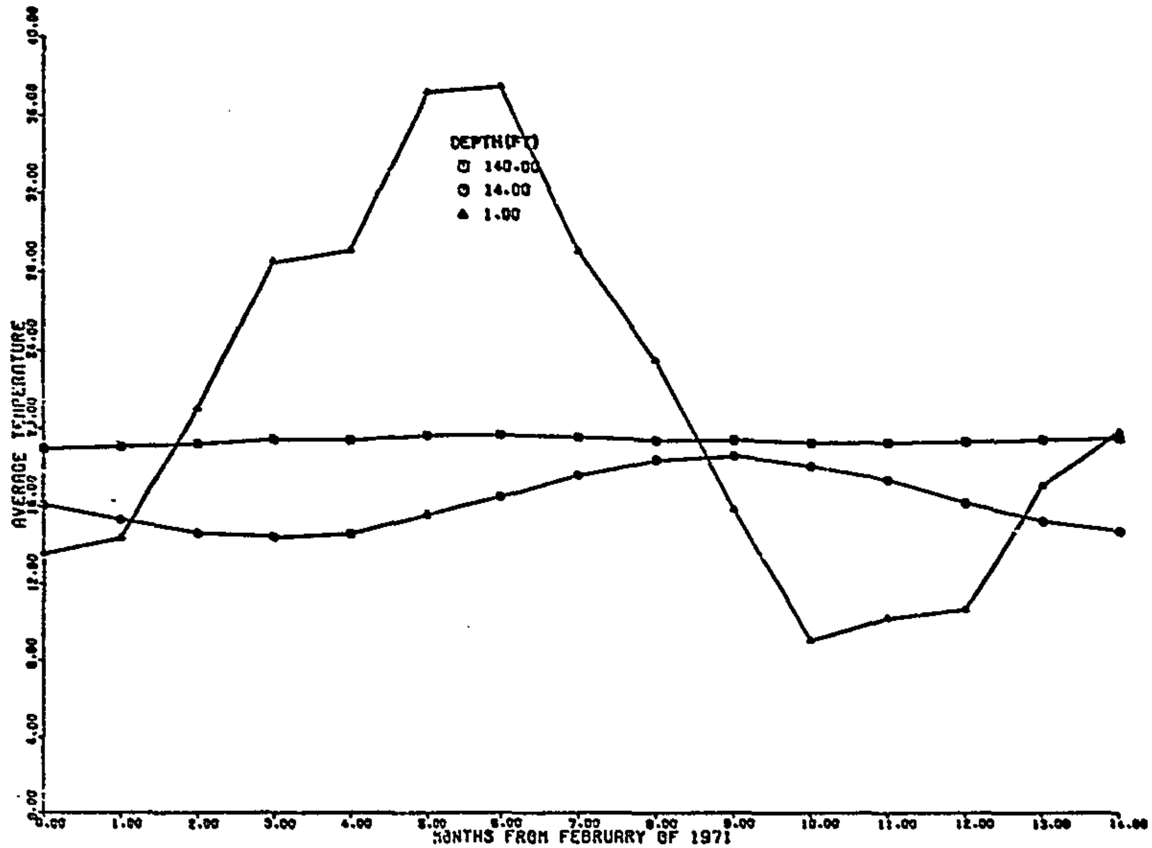

FIGURE D-22. Average Measured Monthly Soil Temperature (°C) Versus Time for Selected Depths

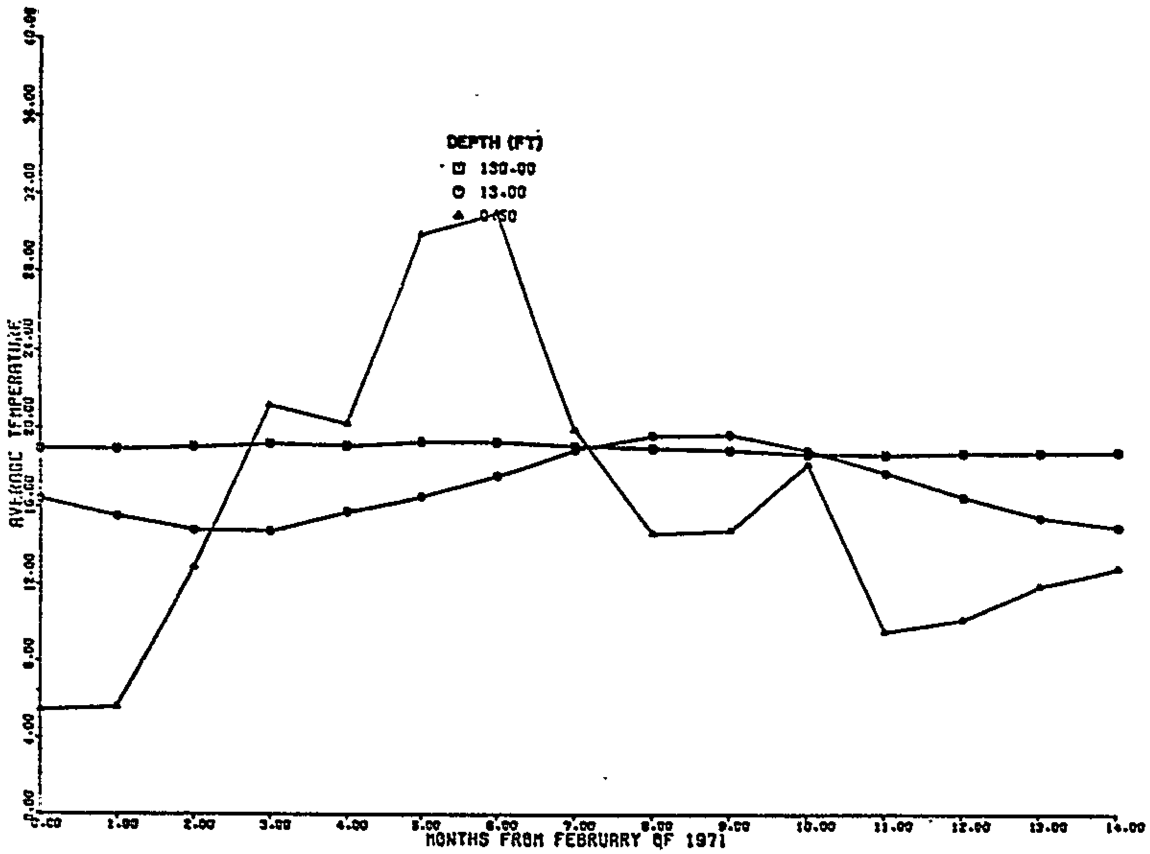

FIGURE D-23. Average Measured Monthly Soil Temperature (°C) Versus Time for Selected Depths